Lawson's criteria for ignition exceeded in an inertial fusion experiment

O. A. Hurricane, A. L. Kritcher, A. B. Zylstra, D. A. Callahan

January 7, 2022

Disclaimer

This document was prepared as an account of work sponsored by an agency of the United States government. Neither the United States government nor Lawrence Livermore National Security, LLC, nor any of their employees makes any warranty, expressed or implied, or assumes any legal liability or responsibility for the accuracy, completeness, or usefulness of any information, apparatus, product, or process disclosed, or represents that its use would not infringe privately owned rights. Reference herein to any specific commercial product, process, or service by trade name, trademark, manufacturer, or otherwise does not necessarily constitute or imply its endorsement, recommendation, or favoring by the United States government or Lawrence Livermore National Security, LLC. The views and opinions of authors expressed herein do not necessarily state or reflect those of the United States government or Lawrence Livermore National Security, LLC, and shall not be used for advertising or product endorsement purposes.

Lawson criterion for ignition exceeded in an inertial fusion experiment[*]

H. Abu-Shawareb,[1] R. Acree,[2] P. Adams,[2] J. Adams,[2] B. Addis,[2] R. Aden,[2] P. Adrian,[3] B. B. Afeyan,[2,4] M. Aggleton,[1] L. Aghaian,[1] A. Aguirre,[2] D. Aikens,[2] J. Akre,[2] F. Albert,[2] M. Albrecht,[2] B. J. Albright,[5] J. Albritton,[2] J. Alcala,[1] C. Alday,Jr.,[1] D. A. Alessi,[2] N. Alexander,[1] J. Alfonso,[1] N. Alfonso,[1] E. Alger,[1] S. J. Ali,[2] Z. A. Ali,[6] W. E. Alley,[2] P. Amala,[2] P. A. Amendt,[2] P. Amick,[2] S. Ammula,[2] C. Amorin,[2] D. J. Ampleford,[7] R. W. Anderson,[2] T. Anklam,[2] N. Antipa,[2] B. Appelbe,[8] C. Aracne-Ruddle,[2] E. Araya,[1] M. Arend,[2] P. Arnold,[2] T. Arnold,[2] J. Asay,[7] L. J. Atherton,[2] D. Atkinson,[2] R. Atkinson,[1] J. M. Auerbach,[2] B. Austin,[1] L. Auyang,[2] J. Ayers,[2] S. Ayers,[2] T. Ayers,[9] S. Azevedo,[2] B. Bachmann,[2] C. A. Back,[1] J. Bae,[1] D. S. Bailey,[2] J. Bailey,[7] T. Baisden,[2] K. L. Baker,[2] H. Baldis[†,2] D. Barber,[1] M. Barberis,[2] D. Barker,[2] A. Barnes,[2] C. W. Barnes,[5] M. A. Barrios,[2] C. Barty,[2] I. Bass,[2] S. H. Batha,[5] S. H. Baxamusa,[2] G. Bazan,[2] J. K. Beagle,[2] R. Beale,[2] B. R. Beck,[2] J. B. Beck,[5] M. Bedzyk,[10] R. G. Beeler(II),[2] R. G. Beeler(III),[2] W. Behrendt,[2] L. Belk,[2] P. Bell,[2] M. Belyaev,[2] J. F. Benage,[7] G. Bennett,[7] L. R. Benedetti,[2] L. X. Benedict,[2] R. Berger,[2] T. Bernat,[2] L. A. Bernstein,[2,11,12] B. Berry,[1] L. Bertolini,[2] G. Besenbruch[†,1] J. Betcher,[9] R. Bettenhausen,[2] R. Betti,[10] B. Bezzerides[†,5] S. D. Bhandarkar,[2] R. Bickel,[2] J. Biener,[2] T. Biesiada,[2] K. Bigelow,[13] J. Bigelow-Granillo,[13] V. Bigman,[7] R. M. Bionta,[2] N. W. Birge,[5] M. Bitter,[14] A. C. Black,[2] R. Bleile,[2] D. L. Bleuel,[2] E. Bliss,[2] E. Bliss,[2] B. Blue,[2] K. Boehm,[1] C. D. Boley,[2] R. Bonanno,[2] E. J. Bond,[2] T. Bond,[2] M. J. Bonino,[10] M. Borden,[2] J.-L. Bourgade,[15] J. Bousquet,[1] J. Bowers,[2] M. Bowers,[2] R. Boyd,[2] A. Bozek,[1] D. K. Bradley,[2] K. S. Bradley,[5] P. A. Bradley,[5] L. Bradley,[1] L. Brannon,[1] P. S. Brantley,[2] D. Braun,[2] T. Braun,[2] K. Brienza-Larsen,[6] T. M. Briggs,[2] J. Britten,[2] E. D. Brooks,[2] D. Browning,[2] M. W. Bruhn,[2] T. A. Brunner,[2] H. Bruns,[2] G. Brunton,[2] B. Bryant,[2] T. Buczek,[10] J. Bude,[2] L. Buitano,[16] S. Burkhart,[2] J. Burmark,[2] A. Burnham,[2] R. Burr,[2] L. E. Busby,[2] B. Butlin,[2] R. Cabeltis,[1] M. Cable,[2] W. H. Cabot,[2] B. Cagadas,[1] J. Caggiano,[2] R. Cahayag,[1] S. E. Caldwell,[5] S. Calkins,[16] D. A. Callahan,[2] J. Calleja-Aguirre,[1] L. Camara,[2] D. Camp,[2] E. M. Campbell,[10] J. H. Campbell,[2] B. Carey,[2] R. Carey,[2] K. Carlisle,[2] L. Carlson,[1] L. Carman,[2] J. Carmichael,[1] A. Carpenter,[2] C. Carr,[2] J. A. Carrera,[2] D. Casavant,[2] A. Casey,[2] D. T. Casey,[2] A. Castillo,[1] E. Castillo,[1] J. I. Castor[†,2] C. Castro,[2] W. Caughey,[1] R. Cavitt,[2] J. Celeste,[2] P. M. Celliers,[2] C. Cerjan,[2] G. Chandler,[7] B. Chang,[2] C. Chang,[2] J. Chang,[2] L. Chang,[2] R. Chapman,[10] T. Chapman,[2] L. Chase,[2] H. Chen,[2] H. Chen,[1] K. Chen,[1] L.-Y. Chen,[2] B. Cheng,[5] J. Chittenden,[8] C. Choate,[2] J. Chou,[2] R. E. Chrien,[5,2] M. Chrisp,[2] K. Christensen,[2] M. Christensen,[2] A. R. Christopherson,[2] M. Chung,[1] J. A. Church,[2] A. Clark,[1] D. S. Clark,[2] K. Clark,[1] R. Clark,[2] L. Claus,[7] B. Cline,[2] J. A. Cline,[2] J. A. Cobble,[5] K. Cochrane,[7] B. Cohen,[2] S. Cohen,[2] M. R. Collette,[2] G. Collins,[10] L. A. Collins,[5] T. J. B. Collins,[10] A. Conder,[17] B. Conrad,[2] M. Conyers[†,1] A. W. Cook,[2] D. Cook,[16] R. Cook,[2] J.C. Cooley,[5] G. Cooper,[7,18] T. Cope,[2] S. R. Copeland,[2] F. Coppari,[2] J. Cortez,[13] J. Cox,[2] D. H. Crandall,[16] J. Crane,[2] R. S. Craxton,[10] M. Cray,[5] A. Crilly,[8] J. W. Crippen,[1] D. Cross,[2] M. Cuneo,[7] G. Cuotts,[2] C. E. Czajka,[2] D. Czechowicz,[1] T. Daly,[2] P. Danforth,[2] R. Darbee,[2] B. Darlington,[2] P. Datte,[1] L. Dauffy,[2] G. Davalos,[2] S. Davidovits,[2] P. Davis,[16] J. Davis,[2] S. Dawson,[2] R. D. Day,[5] T. H. Day,[5] M. Dayton,[2] C. Deck,[1] C. Decker,[2] C. Deeney,[16] K. A. DeFriend,[5] G. Deis,[2] N. D. Delamater,[5] J. A. Delettrez,[10] R. Demaret,[2] S. Demos,[2] S. M. Dempsey,[2] R. Desjardin,[2] T. Desjardins,[5] M. P. Desjarlais,[7] E. L. Dewald,[2] J. DeYoreo,[2] S. Diaz,[1] G Dimonte,[2,5] T. R. Dittrich,[2] L. Divol,[2] S. N. Dixit,[2] J. Dixon,[2] E. S. Dodd,[5] D. Dolan,[7] A. Donovan,[2] M. Donovan,[16] T. Döppner,[2] C. Dorrer,[10] N. Dorsano,[1] M.R. Douglas,[5] D. Dow,[9] J. Downie,[2] E. Downing,[2] M. Dozieres,[1] V. Draggoo,[2] D. Drake,[16] R. P. Drake,[2,19] T. Drake,[1] G. Dreifuerst,[2] D. F. DuBois,[5] P. F. DuBois,[2] G. Dunham,[7] R. Dylla-Spears,[2] A. K. L. Dymoke-Bradshaw,[20] B. Dzenitis,[2] C. Ebbers,[2] M. Eckart,[2] S Eddinger,[1] D. Eder,[2] D. Edgell,[10] M. J. Edwards,[2] P. Efthimion,[14] J. H. Eggert,[2] B. Ehrlich,[2] P. Ehrmann,[2] S. Elhadj,[2] C. Ellerbee,[2] N. S. Elliott,[2] C. L. Ellison,[2] F. Elsner,[1] M. Emerich,[1] K. Engelhorn,[1] T. England,[7] E. English,[2] P. Epperson,[2] R. Epstein,[10] G. Erbert,[2] M. A. Erickson,[2] D. J. Erskine,[2] A. Erlandson,[2] R. J. Espinosa,[1] C. Estes,[2] K. G. Estabrook[†,2] S. Evans,[5] A. Fabyan,[1] J. Fair,[2] R. Fallejo,[2] N. Farmer,[1] W. A. Farmer,[2] M. Farrell,[1] V. E. Fatherley,[5] M. Fedorov,[2] E. Feigenbaum,[2] M. Feit,[2] W. Ferguson,[2] J. C. Fernandez,[5] A. Fernandez-Panella,[2] S. Fess,[1] J. E. Field,[2] C. V. Filip,[2] J. R. Fincke,[5] T. Finn,[16] S.M. Finnegan,[5] R. G. Finucane,[2] M. Fischer,[2] J. Fisher,[2] B. Fishler,[2] D. Fittinghoff,[2] P. Fitzsimmons,[1] M. Flegel,[2] K. A. Flippo,[5] J. Florio,[1] J. Folta,[2] P. Folta,[2] L. R. Foreman[†,5] C. Forrest,[10] A. Forsman,[1] J. Fooks,[1] M. Foord,[2] R. Fortner,[2] K. Fournier,[2] D. E. Fratanduono,[2] N. Frazier,[16] T. Frazier,[2] C. Frederick,[1] J. Frenje,[3] D. Frey,[1] G. Frieders,[2] S. Friedrich,[2] D. H. Froula,[10] J. Fry,[2] T. Fuller,[1] J. Gaffney,[2] S. Gales,[21] B. Le Galloudec,[2] K. K. Le Galloudec,[2] A. Gambhir,[2] L. Gao,[14] W. J. Garbett,[21] A. Garcia,[1] C. Gates,[2] E. Gaut,[1] P. Gauthier,[15] Z. Gavin,[1] J. Gaylord,[2] M.

Geissel,[7] F. Génin,[2] J. Georgeson,[7] H. Geppert-Kleinrath,[5] V. Geppert-Kleinrath,[5] N. Gharibyan,[2] J. Gibson,[1] C. Gibson,[1] E. Giraldez,[1] V. Glebov,[10] S. G. Glendinning,[2] S. Glenn,[2] S. H. Glenzer,[2,17] S. Goade,[1] P. L. Gobby,[5] S. R. Goldman,[5] B. Golick,[2] M. Gomez,[7] V. Goncharov,[10] D. Goodin,[1] P. Grabowski,[2] E. Grafil,[2] P. Graham,[21] J. Grandy,[2] E. Grasz,[2] F. Graziani,[2] G. Greenman†,[2] J. A. Greenough,[2] A. Greenwood,[1] G. Gregori,[22] T. Green,[2] J. R. Griego,[5] G. P. Grim,[2] J. Grondalski,[2] S. Gross,[13] J. Guckian,[9] N. Guler,[23] B. Gunney,[2] G. Guss,[2] S. Haan,[2] J. Hackbarth,[1] L. Hackel,[2] R. Hackel,[2] C. Haefner,[2,24,25] C. Hagmann,[2] K. D. Hahn,[2] S. Hahn,[2] B. J. Haid,[2] B. M. Haines,[5] B. M. Hall,[2] C. Hall,[7] G. N. Hall,[2] M. Hamamoto,[2] S. Hamel,[2] C. E. Hamilton,[5] B. A. Hammel,[2] J. H. Hammer,[2] G. Hampton,[2] A. Hamza,[2] A. Handler,[2] S. Hansen,[7] D. Hanson,[7] R. Haque,[2] D. Harding,[10] E. Harding,[7] J. D. Hares,[20] D. B. Harris,[5] J. A. Harte,[2] E. P. Hartouni,[2] R. Hatarik,[2] S. Hatchett,[2] A. A. Hauer,[5] M. Havre,[1] R. Hawley,[2] J. Hayes,[1] J. Hayes†,[2] S. Hayes,[2] A. Hayes-Sterbenz,[5] C. A. Haynam,[2] D. A. Haynes,[5] D. Headley,[7] A. Heal,[2] J. E. Heebner,[2] S. Heerey,[2] G. M Heestand†,[2] R. Heeter,[2] N. Hein,[1] C. Heinbockel,[1] C. Hendricks,[2] M. Henesian,[2] J. Heninger,[2] J. Henrikson,[2] E. A. Henry,[2] E. B. Herbold,[2] M. R. Hermann,[2] G. Hermes,[2] J. E. Hernandez,[2] V. J. Hernandez,[2] M. C. Herrmann,[2] H. W. Herrmann,[5] O. D. Herrera,[2] D. Hewett†,[2] R. Hibbard,[2] D. G. Hicks,[2,26] D. Hill,[1] K. Hill,[14] T. Hilsabeck,[1] D. E. Hinkel,[2] D. D. Ho,[2] V. K. Ho,[1] J. K. Hoffer,[5] N. M. Hoffman,[5] M. Hohenberger,[2] M. Hohensee,[2] W. Hoke,[1] D. Holdener,[2] F. Holdener,[2] J. P. Holder,[2] B. Holko,[1] D. Holunga,[2] J. F. Holzrichter,[2] J. Honig,[2] D. Hoover,[1] D. Hopkins,[2] L. Berzak Hopkins,[2] M. Hoppe,Jr.,[1] M. L. Hoppe,Sr.,[1] J. Horner,[2] R. Hornung,[2] C. J. Horsfield,[21] J. Horvath,[2] D. Hotaling,[2] R. House,[2] L. Howell,[2] W. W. Hsing,[2] S. X. Hu,[10] H. Huang,[1] J. Huckins,[2] H. Hui,[2] K. D. Humbird,[2] J. Hund,[1] J. Hunt,[2] O. A. Hurricane*,[2] M. Hutton,[2] K. H.-K. Huynh,[2] L. Inandan,[1] C. Iglesias,[2] I. V. Igumenshchev,[10] N. Izumi,[2] M. Jackson,[1] J. Jackson,[2] S. D. Jacobs†,[10] G. James,[2] K. Jancaitis,[2] J. Jarboe,[2] L. C. Jarrott,[2] D. Jasion,[1] J. Jaquez,[1] J. Jeet,[2] A. E. Jenei,[2] J. Jensen,[1] J. Jimenez,[2] R. Jimenez,[1] D. Jobe,[16] Z. Johal,[1] H. M. Johns,[5] D. Johnson,[7] M. A. Johnson,[2] M. Gatu Johnson,[3] R. J. Johnson,[2] S. Johnson,[2] S. A. Johnson,[2] T. Johnson,[3] K. Jones,[7] O. Jones†,[2] M. Jones,[7] R. Jorge,[1] H. J. Jorgenson,[5] M. Julian,[1] B.I. Jun,[2] R. Jungquist,[10] J. Kaae,[1] N. Kabadi,[3] D. Kaczala,[1] D. Kalantar,[2] K. Kangas,[1] V. V. Karasiev,[10] M. Karasik,[27] V. Karpenko,[2] A. Kasarky,[16] K. Kasper,[2] R. Kauffman,[2] M. I. Kaufman,[6] C. Keane,[2,28] L. Keaty,[1] L. Kegelmeyer,[2] P. A. Keiter,[5] P. A. Kellett,[20] J. Kellogg,[7] J. H. Kelly,[10] S. Kemic,[5] A. J. Kemp,[2] G. E. Kemp,[2] G. D. Kerbel,[2] D. Kershaw,[2] S. M. Kerr,[2] T. J. Kessler,[10] M. H. Key,[2] S. F. Khan,[2] H. Khater,[2] C. Kiikka,[2] J. Kilkenny,[1] Y. Kim,[5] Y.-J. Kim,[2] J. Kimko,[2] M. Kimmel,[7] J. M. Kindel,[16] J. King,[2] R. K. Kirkwood,[2] L. Klaus,[2] D. Klem,[2] J. L. Kline,[5] J. Klingmann,[2] G. Kluth,[15] P. Knapp,[7] J. Knauer,[10] J. Knipping,[1] M. Knudson,[7] D. Kobs,[1] J. Koch†,[2] T. Kohut,[2] C. Kong,[1] J. M. Koning,[2] P. Koning,[2] S. Konior,[1] H. Kornblum,[2] L. B. Kot,[5] B. Kozioziemski,[2] M. Kozlowski,[2] P. M. Kozlowski,[5] J. Krammen,[2] N. S. Krasheninnikova,[5] B. Kraus,[14] W. Krauser,[5] J. D. Kress,[5] A. L. Kritcher,[2] E. Krieger,[2] J. J. Kroll,[2] W. L. Kruer,[2] M. K. G. Kruse,[2] S. Kucheyev,[2] M. Kumbera,[2] S. Kumpan,[2] J. Kunimune,[3] B. Kustowski,[2] T. J. T. Kwan,[5] G. A. Kyrala,[5] S. Laffite,[15] M. Lafon,[15] K. LaFortune,[17] B. Lahmann,[3,2] B. Lairson,[9] O. L. Landen,[2] J. Langenbrunner,[5] L. Lagin,[2] T. Land,[2] M. Lane,[2] D. Laney,[2] A. B. Langdon,[2] S. H. Langer,[2] A. Langro,[2] N. E. Lanier,[5] T. E. Lanier,[2] D. Larson,[2] B. F. Lasinski,[2] D. Lassle,[2] D. LaTray,[2] G. Lau,[2] N. Lau,[1] C. Laumann,[2] A. Laurence,[1] T. A. Laurence,[2] J. Lawson,[6] H. P. Le,[2] L. Leal,[1] A. Leatherland,[21] K. LeChien,[2] B. Lechleiter,[2] A. Lee,[2] M. Lee,[1] T. Lee,[1] R. J. Leeper,[5] E. Lefebvre,[15] J.-P. Leidinger,[15] B. LeMire,[2] R. W. Lemke,[7] N. C. Lemos,[2] S. Le Pape,[2,29] R. Lerche,[2] S. Lerner,[2] S. Letts,[2] K. Levedahl,[16] T. Lewis,[2] C. K. Li,[3] H. Li,[2] J. Li,[2] W. Liao,[2] Z. M. Liao,[2] D. Liedahl,[2] J. Liebman,[2] G. Lindford,[2] E. L. Lindman,[5] J. D. Lindl,[2] H. Loey,[2] R. A. London,[2] F. Long,[7] E. N. Loomis,[5] F. E. Lopez,[5] H. Lopez,[9] E. Losbanos,[1] S. Loucks,[10] R. Lowe-Webb,[2] E. Lundgren,[1] A. P. Ludwigsen,[2] R. Luo,[1] J. Lusk,[2] R. Lyons,[2] T. Ma,[2] Y. Macallop,[13] M. J. MacDonald,[2] B. J. MacGowan,[2] J. M. Mack,[5] A. J. Mackinnon,[2] S. A. MacLaren,[2] A. G. MacPhee,[2] G. R. Magelssen,[5] J. Magoon,[10] R. M. Malone,[6] T. Malsbury,[2] R. Managan,[2] R. Mancini,[30] K. Manes,[2] D. Maney†,[2] D. Manha,[2] O. M. Mannion,[7] A. M. Manuel,[2] E. Mapoles,[2] G. Mara,[2] T. Marcotte,[1] E. Marin,[1] M. M. Marinak,[2] C. Mariscal,[1] D. A. Mariscal,[2] E. F. Mariscal,[2] E. V. Marley,[2] J. A. Marozas,[10] R. Marquez,[1] C. D. Marshall,[2] F. J. Marshall,[10] M. Marshall,[10] S. Marshall,[16] J. Marticorena,[2] D. Martinez,[2] I. Maslennikov,[2] D. Mason,[2] R. J. Mason,[5] L. Masse,[2,15] W. Massey,[2] P.-E. Masson-Laborde,[15,31] D. Mathisen,[2] E. Mathison,[1] J. Matone,[2] M. J. Matthews,[2] C. Mattoon,[2] T. R. Mattsson,[7] K. Matzen,[7] C. W. Mauche,[2] M. Mauldin,[1] T. McAbee,[2] M. McBurney,[2] T. Mccarville,[2] R. L. McCrory,Jr.,[10] A. M. McEvoy,[5] C. McGuffey,[1] M. Mcinnis,[1] P. McKenty,[10] M. S. McKinley,[2] J. B. McLeod,[2] A. McPherson,[7] B. Mcquillan†,[1] M. Meamber,[2] K. D. Meaney,[5] N. B. Meezan,[2] R. Meissner,[2] T. A. Mehlhorn,[7] N. C. Mehta,[2] J. Menapace,[2] F. E. Merrill,[5] B. T. Merritt,[2] E. C. Merritt,[5] D. D. Meyerhofer,[5] S. Mezyk,[2] R. J. Mich,[2] P. A. Michel,[2] D. Milam,[2] C. Miller,[2] D. Miller,[2] D. S. Miller,[2]

E. Miller,[2] E. K. Miller,[6] J. Miller†,[2] M. Miller,[2] P. E. Miller,[2] T. Miller,[1] W. Miller,[1] V. Miller-Kamm,[2] M. Millot,[2] J. L. Milovich,[2] P. Minner,[2] J.-L. Miquel,[15] S. Mitchell,[2] K. Molvig,[5] R. C. Montesanti,[2] D. S. Montgomery,[5] M. Monticelli,[2] A. Montoya,[7] J. D. Moody,[2] A. S. Moore,[2] E. Moore,[2] M. Moran,[2] J. C. Moreno,[2] K. Moreno,[1] B. E. Morgan,[2] T. Morrow,[5] J. W. Morton,[21] E. Moses,[2] K. Moy,[6] R. Muir,[2] M. S. Murillo,[2,32] J. E. Murray,[2] J. R. Murray†,[2] D. H. Munro,[2] T. J. Murphy,[5] F. M. Munteanu,[2] J. Nafziger,[1] T. Nagayama,[7] S. R. Nagel,[2] R. Nast,[1] R. A. Negres,[2] A. Nelson,[7] D. Nelson,[10] J. Nelson,[2] S. Nelson,[16] S. Nemethy,[2] P. Neumayer,[2,33] K. Newman,[2] M. Newton,[2] H. Nguyen,[2] J.-M. G. Di Nicola,[2] P. Di Nicola,[2] C. Niemann,[2,34] A. Nikroo,[2] P. M. Nilson,[10] A. Nobile,[5] V. Noorai,[1] R. Nora,[2] M. Norton,[2] M. Nostrand,[2] V. Note,[2] S. Novell,[2] P. F. Nowak,[2] A. Nunez,[1] R. A. Nyholm,[2] M. O'Brien,[2] A. Oceguera,[2] J. A. Oertel,[5] J. Okui,[2] B. Olejniczak,[2] J. Oliveira,[2] P. Olsen,[2] B. Olson,[2] K. Olson,[2] R. E. Olson,[5] Y. P. Opachich,[2] N. Orsi,[2] C. D. Orth,[2] M. Owen,[2] S. Padalino,[2,35] E. Padilla,[2] R. Paguio,[1] S. Paguio,[1] J. Paisner,[5] S. Pajoom,[1] A. Pak,[2] S. Palaniyappan,[5] K. Palma,[2] T. Pannell,[2] F. Papp,[2] D. Paras,[1] T. Parham,[2] H.-S. Park,[2] A. Pasternak,[13] M. Patankar,[2] M. V. Patel,[2] P. K. Patel,[2,36] R. Patterson,[2] S. Patterson,[2] B. Paul,[9] M. Paul,[2] E. Pauli,[2] O. T. Pearce,[2] J. Pearcy,[3] B. Pedrotti,[2] A. Peer,[2] L. J. Pelz,[2] B. Penetrante†,[2] J. Penner,[2] A. Perez,[1] L. J. Perkins,[2] E. Pernice,[2] T. S. Perry,[5] S. Person,[2] D. Petersen,[2] T. Petersen,[2] D. L. Peterson†,[5] E. B. Peterson,[1] J. E. Peterson,[2] J. L. Peterson,[2] K. Peterson,[7] R. R. Peterson,[5] R. D. Petrasso,[3] F. Philippe,[15] T. J. Phipps,[1] E. Piceno,[1] Y. Ping,[2] L. Pickworth,[37] J. Pino,[2] R. Plummer,[2] G. D. Pollack,[5] S. M. Pollaine,[2] B. B. Pollock,[2] D. Ponce,[1] J. Ponce,[1] J. Pontelandolfo,[1] J. L. Porter,[7] J. Post,[2] O. Poujade,[15,31] C. Powell,[2] H. Powell†,[2] G. Power,[2] M. Pozulp,[2] M. Prantil,[2] M. Prasad,[2] S. Pratuch,[2] S. Price,[1] K. Primdahl,[2] S. Prisbrey,[2] R. Procassini,[2] A. Pruyne,[10] B. Pudliner,[2] S. R. Qiu,[2] K. Quan,[1] M. Quinn,[1] J. Quintenz,[1] P. B. Radha,[10] F. Rainer,[2] J. E. Ralph,[2] K. S. Raman,[2] R. Raman,[2] P. Rambo,[7] S. Rana,[2] A. Randewich,[21] D. Rardin,[2] M. Ratledge,[1] N. Ravelo,[1] F. Ravizza,[2] M. Rayce,[2] A. Raymond,[1] B. Raymond,[2] B. Reed,[2] C. Reed,[1] S. Regan,[10] B . Reichelt,[3] V. Reis,[16] S. Reisdorf,[2] V. Rekow,[2] B. A. Remington,[2] A. Rendon,[2] W. Requieron,[1] M. Rever,[2] H. Reynolds,[1] J. Reynolds,[1] J. Rhodes,[2] M. Rhodes,[2] M. C. Richardson,[10,38] B. Rice,[10] N. G. Rice,[1] R. Rieben,[2] A. Rigatti,[10] S. Riggs,[2] H. G. Rinderknecht,[10] K. Ring,[1] B. Riordan,[1] R. Riquier,[15] C. Rivers,[1] D. Roberts,[2] V. Roberts,[2] G. Robertson,[7] H. F. Robey,[5] J. Robles,[1] P. Rocha,[2] G. Rochau,[7] J. Rodriguez,[1] S. Rodriguez,[2] M. Rosen,[2] M. Rosenberg,[10] G. Ross,[2] J. S. Ross,[2] P. Ross,[16] J. Rouse,[2] D. Rovang,[7] A. M. Rubenchik,[2] M. S. Rubery,[2] C. L. Ruiz,[7] M. Rushford,[2] B. Russ,[1] J. R. Rygg,[10] B. S. Ryujin,[2] R. A. Sacks,[2] R. F. Sacks,[5] K. Saito,[1] T. Salmon,[2] J. D. Salmonson,[2] J. Sanchez,[2] S. Samuelson,[16] M. Sanchez,[7] C. Sangster,[10] A. Saroyan,[2] J. Sater,[2] A. Satsangi,[16] S. Sauers,[2] R. Saunders,[2] J. P. Sauppe,[5] R. Sawicki,[2] D. Sayre,[2] M. Scanlan,[2] K. Schaffers,[2] G. T. Schappert,[5] S. Schiaffino†,[2] D. J. Schlossberg,[2] D. W. Schmidt,[5] M. J. Schmitt,[5] D. H. G. Schneider,[2] M. B. Schneider,[2] R. Schneider,[16] M. Schoff,[1] M. Schollmeier,[7] C. R. Schroeder,[2] S. E. Schrauth,[2] H. A. Scott,[2] I. Scott,[1] J. M. Scott,[5] R. H. H. Scott,[39] C. R. Scullard,[2] T. Sedillo,[5] F. H. Seguin,[3] W. Seka,[10] J. Senecal,[2] S. M. Sepke,[2] L. Seppala,[2] K. Sequoia,[1] J. Severyn,[2] J. M. Sevier,[2] N. Sewell,[2] S. Seznec,[15] R. C. Shah,[10] J. Shamlian,[10] D. Shaughnessy,[2] M. Shaw,[2] R. Shaw,[2] C. Shearer,[1] R. Shelton,[2] N. Shen,[2] M. W. Sherlock,[2] A. I. Shestakov,[2] E. L. Shi,[2] S. J. Shin,[2] N. Shingleton,[2] W. Shmayda,[10] M Shor,[2] M. Shoup,[10] C. Shuldberg,[1] L. Siegel,[2] F. J. Silva,[1] A. N. Simakov,[5] D. Sinars,[7] P. Singh,[1] H. Sio,[3,2] K. Skulina,[2] S. Skupsky,[10] S. Slutz,[7] M. Sluyter,[16] V. A. Smalyuk,[2] D. Smauley,[2] R. M. Smeltser,[7] C. Smith,[2] I. Smith,[7] J. Smith,[1] L. Smith,[2] R. Smith,[9] M. Schölmerich,[2] R. Sohn,[1] S. Sommer,[2] C. Sorce,[10] M. Sorem,[5] J. M. Soures,[10] M. L. Spaeth,[2] B. K. Spears,[2] S. Speas,[7] D. Speck,[2] R. Speck,[2] J. Spears,[2] T. Spinka,[2] P. T. Springer,[2] M. Stadermann,[2] B. Stahl,[1] J. Stahoviak,[7] L. G. Stanton,[2,40] R. Steele,[2] W. Steele†,[2] D. Steinman†,[1] R. Stemke,[1] R. Stephens,[1] S. Sterbenz,[6] P. Sterne,[2] D. Stevens,[2] J. Stevers,[2] C. B. Still†,[2] C. Stoeckl,[10] W. Stoeffl,[2] C. Stolz,[2] E. Storm,[2] G. Stone,[2] S. Stoupin,[2] E. Stout,[2] I. Stowers,[2] R. Strauser,[1] H. Streckart,[1] J. Streit,[13] D. J. Strozzi,[2] T. Suratwala,[2] G. Sutcliffe,[3] L. J. Suter,[2] S. B. Sutton,[2] V. Svidzinski,[2] G. Swadling,[2] W. Sweet,[1] A. Szoke†,[2] M. Tabak,[2] M. Takagi,[2] A. Tambazidis,[1] V. Tang,[2] M. Taranowski,[2] L. A. Taylor,[2] S. Telford,[2] W. Theobald,[10] M. Thi,[1] A. Thomas,[2] C. A. Thomas,[2,10] I. Thomas†,[2] R. Thomas†,[7] I. J. Thompson,[2] A. Thongstisubskul,[1] C. B. Thorsness,[2] G. Tietbohl,[2] R. E. Tipton,[2] N. Tomlin,[1] R. Tommasini,[2] A. J. Toreja,[2] J. Torres,[7] R. P. J. Town,[2] S. Townsend,[2] J. Trenholme†,[2] A. Trivelpiece,[2] C. Trosseille,[2] H. Truax,[1] D. Trummer,[2] S. Trummer,[2] T. Truong,[16] D. Tubbs,[5] E. R. Tubman,[2] T. Tunnell,[6] D. Turnbull,[10] R. E. Turner,[2] M. Ulitsky,[2] R. Upadhye,[2] J. L. Vaher,[2] P. VanArsdall,[2] D. VanBlarcom,[2] M. Vandenboomgaerde,[15] R. VanQuinlan,[2] B. M. Van Wonterghem,[2] W. S. Varnum,[5] A. L. Velikovich,[27] A. Vella,[2] C. P. Verdon,[16] B. Vermillion,[1] S. Vernon,[2] R. Vesey,[7] J. Vickers,[1] M. Visosky,[16] J. Vocke,[1] P. L. Volegov,[5] S. Vonhof,[1] R. Von Rotz,[2] H. X. Vu,[5] M. Vu,[1] D. Wall,[1] J. Wall,[1] R. Wallace,[2] B. Wallin,[2] D. Walmer,[2] C. A. Walsh,[2] C. F. Walters,[2] C. Waltz,[2] A. Wan,[2] A. Wang,[2] Y.

Wang,[2] J. S. Wark,[22] B. E. Warner,[2] J. Watson,[2] R. G. Watt,[5] P. Watts,[2] J. Weaver,[27] R. P. Weaver,[5] S. Weaver,[2] C. R. Weber,[2] P. Weber,[2] S. V. Weber,[2] P. Wegner,[2] B. Welday,[2] L. Welser-Sherrill,[5] K. Weiss,[2] K. Widmann,[2] G. F. Wheeler,[2] W. Whistler[†],[2] R. K. White,[2] H. D. Whitley,[2] P. Whitman,[2] M. E. Wickett,[2] C. Widmayer,[2] J. Wiedwald,[2] R. Wilcox,[12] S. Wilcox,[2] C. Wild,[41] B. H. Wilde,[5] C. H. Wilde,[5] K. Wilhelmsen,[2] M. D. Wilke[†],[5] H. Wilkens,[1] P. Wilkins,[2] S. C. Wilks,[2] E. A. Williams,[2] G. J. Williams,[2] W. Williams,[2] W. H. Williams,[2] D. C. Wilson,[5] B. Wilson,[2] E. Wilson,[2] R. Wilson,[2] S. Winters,[2] J. Wisoff,[2] M. Wittman,[10] J. Wolfe,[2] A. Wong,[2] K. W. Wong,[2] L. Wong,[2] N. Wong,[2] R. Wood,[2] D. Woodhouse,[1] J. Woodruff[†],[2] D. T. Woods,[2] S. Woods,[1] B. N. Woodworth,[2] E. Wooten,[1] K. Work,[6] J. B. Workman,[5] J. Wright,[2] M. Wu,[7] C. Wuest,[6] F. J. Wysocki,[5] H. Xu,[1] M. Yamaguchi,[1] B. Yang,[2] S. T. Yang,[2] J. Yatabe,[2] C. B.Yeamans,[2] B. C. Yee,[2] S.A. Yi,[5] L. Yin,[5] B. Young,[2] C. S. Young,[5] C. V. Young,[2] P. Young,[2] K. Youngblood,[1] R. Zacharias,[2] G. Zagaris,[2] N. Zaitseva,[2] F. Zaka,[2] F. Ze,[2] B. Zeiger,[9] M. Zika,[2] G. B. Zimmerman,[2] T. Zobrist,[2] J. D. Zuegel,[10] and A. B. Zylstra[2]

[1]*General Atomics, San Diego, California 92186, USA*
[2]*Lawrence Livermore National Laboratory, P.O. Box 808, Livermore, California 94551-0808, USA*
[3]*Massachusetts Institute of Technology, Cambridge, Massachusetts 02139, USA*
[4]*Polymath Research Inc., 827 Bonde Ct., Pleasanton, CA 94566*
[5]*Los Alamos National Laboratory, Mail Stop F663, Los Alamos, New Mexico 87545, USA*
[6]*Nevada National Security Site, 232 Energy Way, North Las Vegas, NV, 89030, USA*
[7]*Sandia National Laboratories, P.O. Box 5800 Albuquerque, New Mexico 87123, USA*
[8]*Imperial College London, Plasma Physics, South Kensington Campus, London, SW7 2AZ, UK*
[9]*Luxel Corporation, P.O. Box 1879, 60 Saltspring Dr., Friday Harbor, WA 98250, USA*
[10]*Laboratory for Laser Energetics, University of Rochester, Rochester, New York 14623, USA*
[11]*University of California at Berkeley, Dept. of Nuclear Engineering,*
4165 Etcheverry Hall, Berkeley, CA 94720-1730, USA
[12]*Lawrence Berkeley National Laboratory, 1 Cyclotron Road, Berkeley, CA 94720, USA*
[13]*Gryphon Technologies, 303 Lindbergh Ave., Livermore, CA 94551, USA*
[14]*Princeton Plasma Physics Laboratory, 100 Stellarator Road, Princeton, NJ 08540, USA*
[15]*CEA/DAM/DIF, 91297 Arpajon cedex, France*
[16]*National Nuclear Security Administration, Office of Defense Programs,*
United States Department of Energy, Washington, DC 20585, USA
[17]*SLAC National Accelerator Laboratory, Menlo Park, California 94025, USA*
[18]*University of New Mexico, Dept. of Nuclear Engineering,*
MSC01 1120, 1 University of New Mexico, Albuquerque, NM 87131-0001
[19]*University of Michigan, Climate & Space Research Building,*
2455 Hayward Street Ann Arbor, MI 48109-2143, USA
[20]*Kentech Instruments Ltd., Isis Building, Howbery Park, Wallingford, Oxfordshire, OX10 8BD, UK*
[21]*Atomic Weapons Establishment, Aldermaston, RG7 4PR, United Kingdom*
[22]*Department of Physics, Clarendon Lab, University of Oxford, Parks Road, Oxford, OX1 3PU, UK*
[23]*Spectral Sciences Inc., 4 Fourth Ave, Burlington, MA 01803-3304, USA*
[24]*Fraunhofer Institute for Laser Technology ILT, 52066 Aachen, Germany*
[25]*RWTH Aachen University, 52066 Aachen, Germany*
[26]*Optical Sciences Centre, Department of Physics and Astronomy,*
Swinburne University of Technology, Hawthorn, Victoria 3122, AU
[27]*United States Naval Research Laboratory, Plasma Physics Division,*
4555 Overlook Ave SW, Washington, DC 20375, USA
[28]*Washington State University, Office of Research,*
P.O. Box 641060, Pullman, WA 99164-1060, USA
[29]*Laboratoire pour l'utilisation des Lasers Intenses chez École Polytechnique, F-91128 Palaiseau cedex, France*
[30]*University of Nevada at Reno, Dept. of Physics,*
MS 0220, 1664 N. Virginia St., Reno, NV 89557, USA
[31]*Université of Paris-Saclay, CEA, LMCE, 91680 Bruyères-le-Châtel, France*
[32]*Department of Computational Mathematics, Science and Engineering,*
Michigan State University, East Lansing, Michigan 48824
[33]*GSI Helmholtzzentrum für Schwerionenforschung GmbH, Planckstrasse 1, 64291 Darmstadt, Germany*
[34]*University of California at Los Angeles, Dept. of Physics & Astronomy,*
475 Portola Plaza, Los Angeles, CA 90095-1547, USA
[35]*SUNY Geneseo, Dept. of Physics & Astronomy,*
Integrated Science Center, Geneseo, NY 14454, USA
[36]*Focused Energy Inc., 11525-B Stonehollow Drive, Suite 200, Austin TX 78758 USA*
[37]*Lund University, MAX IV Laboratory, Box 118, 221 00 Lund, Sweden*
[38]*Townes Laser Institute, University of Central Florida, Orlando, FL 32816, USA*
[39]*Central Laser Facility, STFC Rutherford Appleton Laboratory, Harwell Oxford, OC11 0QX, UK*

[40] *Dept. of Mathematics and Statistics, San Jose State University, San Jose, California 95192, USA*
[41] *Diamond Materials Gmbh, 79108 Freiburg, Germany*

For more than half a century, researchers around the world have been engaged in attempts to achieve fusion ignition as a proof of principle of various fusion concepts. Following the Lawson criterion, an ignited plasma is one where the fusion heating power is high enough to overcome all the physical processes that cool the fusion plasma, creating a positive thermodynamic feedback loop with rapidly increasing temperature. In inertially confined fusion, ignition is a state where the fusion plasma can begin "burn propagation" into surrounding cold fuel, enabling the possibility of high energy gain. While "scientific breakeven" (i.e. unity target gain) has not yet been achieved (here target gain is 0.72, 1.37 MJ of fusion for 1.92 MJ of laser energy), this Letter reports the first controlled fusion experiment, using laser indirect-drive, on the National Ignition Facility to produce capsule gain (here 5.8) and reach ignition by nine different formulations of the Lawson criterion.

Nuclear fusion reactions combine two light nuclei into a heavier one, releasing substantial energy in the process. Approaches to generating energy production from fusion typically use thermal reactions (where electron temperature, T_e, and ion temperature, T_i, are similar); in order for copious reactions to occur the fuel must be at extremely high ion temperatures, on the order of several keV (where 1 keV = 1.16×10^7 K). The fundamental challenge of fusion is that while the fusion reactions can self-heat the plasma, at these temperatures the plasma also rapidly loses energy via cooling mechanisms, such as the x-ray radiation that is emitted by the bremsstrahlung process. Early researchers recognized that the most favored fusion reaction is deuterium(D)-tritium(T) fusion [D+T →n (14.1 MeV)+^{4}He (3.5 MeV)] [1] because it has the lowest temperature, ≈ 4.3 keV, at which fusion self-heating power just balances losses from bremsstrahlung x-ray radiation. Additional energy loss mechanisms, such as heat conduction, also cool the plasma, requiring higher temperatures than 4.3 keV to achieve 'ignition', which is when the self-heating overpowers all loss mechanisms ("Lawson-like" ignition criteria) [2] and the temperature rises through a positive thermodynamic instability, resulting in an increasing fusion burn. Such conditions occur in nature in novae and type-1a supernovae, or terrestrially in thermonuclear weapon explosions. Ignition is a step beyond a "burning plasma," where self-heating exceeds the external energy input to heat the plasma as had been recently achieved [3, 4]. This Letter reports on the culmination of a decade effort in inertial confinement fusion (ICF) on the National Ignition Facility (NIF) [5] that resulted in an igniting implosion with over a MJ fusion yield putting ICF on the threshold of unity gain in the laboratory for the first time. This is the first controlled fusion experiment to exceed Lawson-like ignition statements.

Ignition is required for net gain and energy applications using the ICF approach; in contrast, ignition may not be required for other approaches to fusion such as magnetic confinement experiments like the ITER experiment[6]. The original idea behind ICF was explored using lasers to focus energy onto a small capsule containing DT fuel and isentropically compress the target to obtain high thermal temperature ($T_{th} \approx T_e \approx T_i$) and pressures [7, 8] (see Ref. [9] for the early history). Here the fusion burn proceeds while contained by the inertia of the fuel itself over a brief period of time. The inertial confinement time (τ) is related to the 'areal density' (ρR as the radial integral of density, $\rho(R)$) of the fuel. Ignition and subsequent burn into the surrounding fuel ("burn propagation") initiates an explosive, but microscopic scale, release of energy.

Instead of directly driving a capsule with lasers, as originally proposed, here we use 'indirect drive'. The indirect-drive approach to ICF[10] drives a high atomic number cavity, a hohlraum (see Fig. 1a), with laser energy, thereby generating a bath of intense x-rays, measured in terms of radiation temperature ($T_{rad} \sim 300$ eV, see Fig. 1b). The capsule placed at the center of the hohlraum (see Fig. 1a) and its outer surface, the ablator, absorbs the x-ray energy (roughly in proportion to the surface area ratio of the capsule to hohlraum) in a thin layer of ionized plasma, generating high ablation pressures (of order hundreds of Mbar) which produces an inward acceleration (implosion) that accelerates the remaining ablator and DT fuel to high velocity. The generation of ablation pressure is accompanied by the generation of inwardly directed shock waves [11], the precise control of which are a key aspect of any modern ICF design [12–15].

The key element of any ICF scheme is the implosion. Implosions are hydrodynamic systems that do mechanical pdV work on the fusion fuel to both compress and heat it to a high energy-density state, triggering thermonuclear reactions. As the fuel implodes at high velocity (v_{imp}) inwardly, the central pressure begins to increase as the fuel decelerates, doing mechanical work in a process termed "stagnation." During stagnation, the implosion kinetic energy is converted into internal energy, increasing the temperature and pressure ($p \approx 0.77\rho T_{th}$ in Gbar, g/cm^3, keV units) in the DT fuel. In "hot-spot ignition" [21] only a small fraction of the total DT fuel ($\sim 1/10$) is initially heated, reducing the internal energy needed to reach the required T_{th} for ignition.

While the NIF can deliver up to 1.9 MJ of laser en-
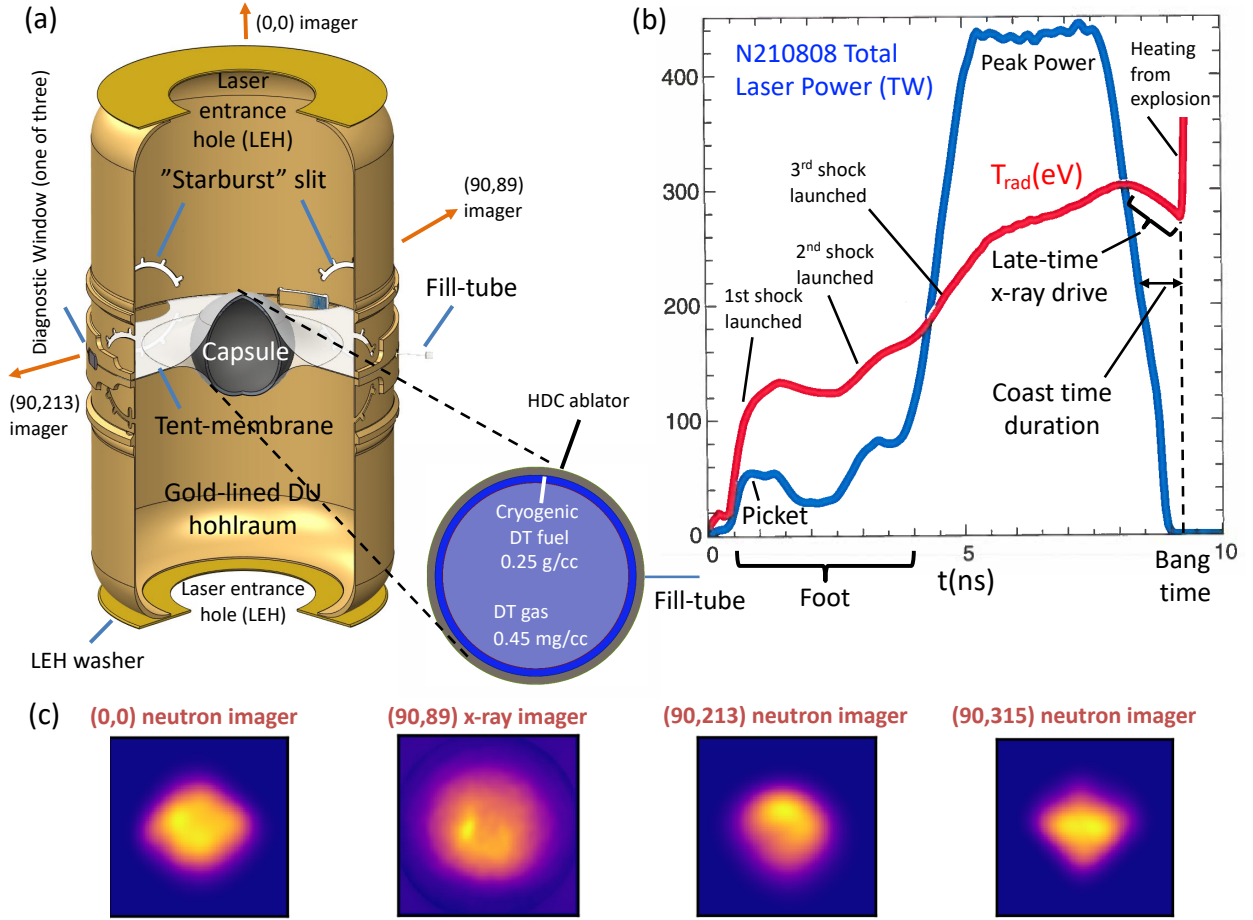
FIG. 1. (a) Cut-away characteristic target geometry [gold-lined depleted uranium hohlraum surrounding an HDC capsule] with some features labeled. The capsule, ~ 2 mm diameter, at the center of the hohlraum, ~ 1 cm height, occupies a small fraction of the volume. Laser beams (not shown) enter the target at the top and bottom apertures called laser entrance holes (LEH's) (outer beams: 44° & 50° inner beams: 23° & 30° relative to the vertical axis of symmetry). The LEH washer forms the LEH aperture. The "starburst" allows imaging of the DT fuel layer during experiment preparation as cryogenic DT liquid is flowed into the capsule via the "fill tube." (b) Total laser power (blue) vs. time and simulated [16] hohlraum radiation temperature (T_{rad}) (red) vs. time for experiment N210808 are shown with a few key elements, discussed in the text, labeled. The "picket" of the laser pulse delivers the first significant burst of energy to the hohlraum and is key to controlling implosion compressibility and hydrodynamic stability. The "foot" of the laser pulse is the duration of the pulse before the rise to peak power – it sets the entropy of the DT fuel via a series of shock waves. The capsule ablation pressure is directly related to T_{rad} and the ablator composition (which in this case is high density carbon, HDC). A key aspect shown is the laser typically turns off ≈ 1 ns before bangtime (denoted "coast-time" duration), of order the hohlraum cooling time [17]. Increasing late-time x-ray drive results in reduced coast-time which enhances the conversion of implosion kinetic energy to DT internal energy [18, 19]. (c) Imaging data from experiments: Neutron images [20] are taken at three lines of sight: (0,0) (technically at $\theta = 5.75$ and $\phi = 225$), (90,315), and (90,213) in target-chamber coordinates [(θ,ϕ) are the respective polar and azimuthal angles measured from the top looking down of the NIF target chamber in degrees]. All images are 100 μm square. Imaging data is used to reconstruct the hotspot plasma volume needed for inferring pressure and other plasma properties.

ergy [5, 22–24] in frequency tripled (351 nm) light to the hohlraum, typically only ~ 20 kJ is converted to fuel kinetic energy because of the inherent inefficiency of the indirect drive approach [10, 15, 25, 26]. This limited energy results in requiring $v_{\mathrm{imp}} \sim 400$ km/s and pressures of hundreds of Gbar [27] to reach the T_{th} and ρR required to initiate substantial self-heating in the central hot spot through deposition of the fusion reaction products (α particles, which are the ^{4}He nuclei). Designing an

implosion that satisfies these conditions, while also controlling hydrodynamic instability (a consequence of the tremendous accelerations/decelerations, $\sim 10^{14-15}$ m/s^2, and material density gradients involved in the implosion) [28] and asymmetry[29–34], requires finesse and engineering control.

Hydrodynamic instability [35–37] can lead to mixing of higher Z (atomic number) capsule ablator material into the fuel and eventually the hot spot, reducing the

ion temperature through radiative cooling [38, 39] that raises the threshold for ignition [40]. Instability can be seeded by fabrication defects on the capsule [41], and by engineering structures such as the support "tent" membrane (see Fig. 1a) that holds the capsule in the center of the hohlraum [42–44] and a 2-10 μm diameter glass tube [45–49] that is inserted into the capsule to fill it with DT fuel. The latter results in a hydrodynamic jet of ablator material entrained into the hot spot resulting in additional radiative cooling [50–52]. Thicker capsules and DT fuel layers are expected to reduce the mixing into the hot spot [53], but this choice lowers the maximum possible implosion velocity, with fixed drive, due to the extra mass. So, with limited laser power and energy available, a more efficient hohlraum [4, 53, 54] is needed to recover implosion velocity.

The NIF commenced layered DT experiments in June 2011 with very high convergence "low-foot" designs using plastic capsules in a high gas-fill (i.e. helium gas-fills of ≥ 0.96 mg/cm^3) hohlraum[15] (see Appendix "History of ICF experiments on the NIF" for a more complete history of key experiments). The 2011-2012 experiments were impacted by high laser-plasma instability (LPI) leading to implosion asymmetry and were more impacted by hydrodynamic instabilities than expected. Stability was improved by using a higher adiabat (i.e. higher DT fuel entropy) 3-shock (see Fig. 1b) high-foot design [28, 55] by raising the power in the "foot" (the first 3-4 ns period before the rise to peak power) of the laser pulse – a tactic that is still used presently (see Fig. 1b). The high foot accessed higher v_{imp}, higher T_{th}, and higher fusion yields with significant α-particle self-heating [56, 57] by systematically reducing coast time thereby increasing late-time ablation pressure (e.g. see Fig. 1b), but asymmetry and the re-emergence of instability as $v_{\mathrm{imp}} \sim 390$ km/s was approached capped performance. High-foot designs used the same hohlraum as the low-foot, albeit with an even higher helium gas-fill of 1.6 mg/cm3 and suffered from similar hohlraum problems. A parallel effort exploring exploding pushers in near vacuum hohlraums, for neutron diagnostic flat-fielding, mitigated losses due to LPI leading to a transition away from high gas-fill hohlraums [58, 59]. Without a high gas-fill, the hohlraum needed to be larger diameter to delay the ingress of hohlraum plasma into the path of the laser beams. HDC ("high density carbon", i.e. industrial diamond) ablators, which are relatively thinner than plastic (for fixed capsule mass because of the density difference of 3.3-3.5 g/^{3} for HDC vs. 1.05 g/^{3} for plastic), allowed for shorter laser pulses which also reduced the ingress of hohlraum plasma. Implosion designs using HDC ablators seemed to tolerate the hydrodynamic perturbations from the tent membrane (a 45 nm thick formvar film that holds the capsule in the center of the hohlraum as shown in Fig. 1a), but are more susceptible to hydrodynamic perturbations from the fill tube (again see Fig. 1a), motivating an engineering effort

to reduce the fill tube diameter. Observed limits [60] on convergence levels with HDC based ablators motivated an alternate strategy using larger capsules to increase energy coupled to the hotspot while not reducing stagnation pressure. With facility limits on maximum laser energy, a simple hydro-scale of all physical dimensions would lead to less x-ray drive resulting in the capsule velocity decreasing and coast for a longer duration, decompressing before stagnation resulting in poor conversion of kinetic energy to hot spot internal energy. Thus the capsule radius was increased, but the thickness was not increased in the same proportion in order to maintain v_{imp} – this was the HYBRID strategy [61–63]. An engineering surprise was apparent when larger radius HDC capsules were first manufactured, exhibiting voids inside the bulk of the shell and pits on the surface of the shell, a problem that challenged an early HYBRID design [64, 65] and is still an engineering problem today. Along with laser improvements (see Appendix on "Laser Improvements"), advances in the understanding of symmetry control in low gas-fill hohlraums, namely an empirical model[66] and extension of cross-beam energy transfer (CBET) tuning to low gas-filled hohlraums through wavelength detuning [67] enabled increasing the capsule scale in more efficient hohlraums.

This Letter reports on work using the HYBRID-E[4, 53, 54] design which increased the amount of energy delivered to the "hot spot" by increasing the capsule radius by 15% compared to previous experiments[64, 68–70]. The challenge of increasing initial capsule radius with fixed laser drive is the potential loss of energy density at the core of the implosion[71]. It is therefore essential to, while increasing the size, maintain the other implosion design parameters including the compressibility of the fuel ('adiabat'), v_{imp}, and the late-time ablation pressure from the drive [18].

In Experiment N210808 (notation being NYYMMDD, N=NIF, YY=year, MM=month, DD=day) that is the focus of this Letter, the late-time ablation pressure was further increased, motivated by a design study which suggested a further improvement in hot spot pressure could be achieved for the HYBRID-E design relative to the previously- reported experiments (N210207 and N210307) [3, 4] through changes made to the hohlraum radiation drive as described in Kritcher *et al.* [16]. In addition, the hydrodynamic stability of the design and the quality of the diamond ablator were both improved.

Hohlraum efficiency was improved by $\sim 15\%$ reducing the diameter of one of the main sources of radiation loss, the laser-entrance-holes (LEH) on both ends of the hohlraum (see Fig. 1a). The reduced LEH diameter was first tested using a gas-filled capsule non-ignition experiment N210601 [72, 73], which verified improved energy coupling with adequate low-mode symmetry. A more efficient hohlraum requires less peak laser power to maintain T_{rad} during most of the laser pulse, and the saved
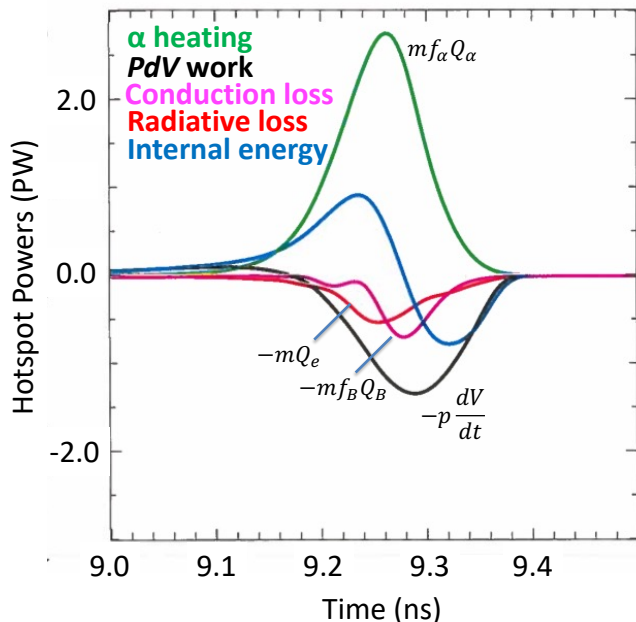
FIG. 2. Simulated hot spot powers of Eq. 1 as a function of time from a model of N210808 [16]. Note that the negative pdV rate of work is a loss comparable to the radiation loss and exceeds the conduction loss, even before peak alpha-heating power is obtained, which is why satisfying the self-heating condition, $f_\alpha Q_\alpha > f_B Q_{B,DT} + Q_e$, is necessary but not sufficient for determining ignition of an ICF implosion. After the time of peak alpha-heating power the negative pdV work is the dominant power loss.

energy was used to extend peak laser power increasing late-time ablation pressure (see Fig. 1b). In-flight implosion radiography data [74] showed that reducing coast time [75, 76] does significantly increase peak v_{imp} and, per theory [18, 19], stagnation pressure by maintaining higher late-time ablation pressure.

Radiation hydrodynamic simulations (HYDRA [77], which itself uses detailed equations of state [78, 79], transport [80, 81], electron-ion coupling [82, 83] and opacity models[84]) was used to calculate these design modifications[16]. The mode-1 radiation flux asymmetry from the low Z diagnostic windows [85], due to their lower albedo, was reduced by a design change to the window sizes and location [32]. The diameter of the capsule fill tube was decreased from 5 to 2 μm to mitigate radiative losses [51] and the number of fabrication defects present in the capsule was reduced by orders of magnitude by fabrication technique and cleanliness improvements.

N210808 the first DT-layered test of these design changes, gave 1.37 MJ fusion yield and that was $8\times$ higher than any previous NIF experiment (and more than $2\times$ the expected yield). The NIF diagnostic suite incorporates significant redundancy as well as detectors utilizing passive media that could be processed appropriately after the shot, a few instruments experienced some level of data saturation. Some electronic data were lost due to neutron shielding being unable to fully mitigate electronics damage, and some instruments required novel analysis methodology to recover their observables. N210808 imaging data (time integrated emission of neutrons and x-rays centered around a photon energy of 13 keV) is shown in Fig. 1c and additional detailed description of instruments and measurement methodology is given in Zylstra et al. [73]. Key scalar data quantities are given in Table 1. Note that post-shot simulations using the delivered laser power and drive asymmetry realized match many measurements for all three experiments reasonably well – see Kritcher, et al. [16].

TABLE I. Key parameters for the experiments highlighted in this Letter are listed. Simulation results can be found in Kritcher et al. [16]. See Zylstra et al. [73] for more detailed diagnostic and experiment descriptions. In order of the list, the parameters are: peak laser power, total laser energy, peak hohlraum radiation temperature (calculated from the measured laser pulse using the method of Ref. 86), coast time (quantitatively defined as mid fall of the laser power to time of peak compression as shown in Fig. 1b), total fusion yield[87–89], neutron time-of-flight[90, 91] inferred temperatures[92], average down scatter ratio ("DSR," the ratio of 10-12 MeV neutrons over 13-15 MeV neutrons registered at the neutron time of flight "NToF" detectors), hot-spot volume (from neutron imaging[20], see Fig. 1c, enclosing 80% of the total yield), measured burn-width (τ_{BW}, which is the full-width-half-maximum duration of gamma ray emission[93]), inferred hot spot burn-average pressure, inferred burn-average hot spot energy, inferred burn-average hot spot areal density (inferred quantities using the method of Ref. 94), fuel gain (ratio of yield to mechanical energy delivered to the DT), capsule gain (ratio of yield to x-ray energy absorbed by the capsule, estimated from post-shot simulations), target gain (ratio of yield to laser energy delivered to the target).

Quantity	$N210207_{Data}$	$N210307_{Data}$	$N210808_{Data}$
P_{laser} (TW)	470	487	441
E_{laser} (MJ)	1.93	1.909	1.917
Peak T_{rad} (eV)	302	294	307
t_{coast} (ns)	1.09	1.26	0.83
Y_{total} (MJ)	0.170	0.145	1.37
T_{DT} (keV)	5.66 ± 0.13	5.55 ± 0.11	10.9 ± 0.4
T_{DD} (keV)	5.23 ± 0.16	4.87 ± 0.14	8.94 ± 0.4
DSR (%)	3.16 ± 0.16	3.49 ± 0.16	2.87 ± 0.24
V ($10^5 \mu m^3$)	3.3 ± 0.3	2.7 ± 0.3	6.4 ± 0.75
τ_{BW} (ps)	103 ± 25	138 ± 20	89 ± 5
p_{hs} (Gbar)	351 ± 23	353 ± 23	569 ± 61
E_{hs} (kJ)	17.4 ± 1.1	14.6 ± 0.9	55 ± 6.0
ρR_{hs} (g/cm^2)	0.37 ± 0.4	0.38 ± 0.02	0.44 ± 0.05
G_{fuel}	$7.5^{+0.54}_{-0.82}$	$7.77^{+0.55}_{-0.82}$	$75.6^{+3.6}_{-5.6}$
$G_{capsule}$	0.75 ± 0.05	0.69 ± 0.05	5.8
G_{target}	0.089	0.075	0.72

The ignition process is fundamentally about power balance. The per unit mass power balance in an ICF plasma that determines the hot spot thermal temperature, T_{th}, is (e.g. see Refs. [62, 63] for the form below)

$$c_{\mathrm{DT}}\frac{dT_{\mathrm{th}}}{dt} = f_\alpha Q_\alpha - f_B Q_{\mathrm{B,DT}} - Q_\mathrm{e} - \frac{1}{m}p\frac{dV}{dt} \qquad (1)$$

where $c_{\mathrm{DT}} = 0.115$ GJ/(g·keV) is the DT plasma heat capacity[95], $Q_\alpha = 8.2 \times 10^{24}\rho\langle\sigma v\rangle$ is heating power per unit mass (m) from α particles produced by fusion (with reaction-rate $\langle\sigma v\rangle$), $Q_{\mathrm{B,DT}} = 3.1 \times 10^7 \rho\sqrt{T_\mathrm{e}}$ is the bremsstrahlung emission per unit mass for an equimolar DT mixture, $Q_\mathrm{e} = 5.4 \times 10^3 T^{3.2}/(\rho^{0.8}R^2)$ or $Q_e = 5.9 \times 10^3 T^{7/2}/(\rho R^2)$ is the electron conduction loss (assuming a SESAME [96] conductivity form or a Spitzer [97] form, respectively), and R is the time-dependent hot-spot radius (Q's in units of in GJ/(g · s)). The term f_B is the fraction of x-rays lost to the hot plasma, which is < 1 if the optical depth of the hot region is high enough to re-absorb x-rays or > 1 if the presence of high-Z material enhances x-ray loss beyond that of pure DT.

In order to self-heat a mass of DT, some of the fusion by-products, ^{4}He (α's), must be stopped by collisions in the plasma, thereby adding internal energy, which in-turn increases T_{th}, the fusion reaction-rate, and the hot-spot mass as additional fuel is ablated into the hot-spot, all resulting in an amplification of fusion yield (Y_{amp}, the factor by which the yield increases above what pdV work alone would have produced). Generally, stopping 14 MeV fusion neutrons is not possible in an ICF hot spot, so it is only the stopping of the α particles that matters. The quantity $f_\alpha \leq 1$ in Eq. 1 is the fraction of alpha-particles stopped in the hot DT plasma and is related to the T_{th} and ρR dependent alpha-stopping distance for which a number of different approximations exist[98]; typical values are $f_\alpha \sim 0.7 - 0.8$. The pdV work term in Eq. 1, is a source of mechanical power injection into the plasma on implosion ($dV/dt < 0$) or a loss term upon explosion ($dV/dt > 0$) as the volume V surrounding the hot plasma changes.

A tipping-point in DT plasma self-heating can be obtained if the $f_\alpha Q_\alpha$ term in Eq. 1 dominates over the other terms on the right-hand-side of the power balance for sufficient time. Models of the hot spot energy partition for N210808, Fig.2, show that the amount of alpha heating energy in the hot spot far outweighs the amount of pdV work done on the hot spot and the loss terms (Bremsstrahlung radiation loss and conduction loss), resulting in a significant increase in hot spot internal energy well beyond the time of explosion (when the pdV power changes sign). Once this tipping-point, "ignition," is reached thermal instability follows and T_{th} increases in a finite-time singular (explosive) fashion over the "bootstrapping" time-scale, dimensionally determined per Eq. 1 by the ratio of heat capacity and alpha heating rate at stagnation (subscript s) namely $dt/d\ln T_{\mathrm{th}} \sim$

$c_{\mathrm{DT}}T_{\mathrm{th}}/(f_\alpha Q_\alpha) \sim 2.9 \times 10^{-6}c_{\mathrm{DT}}/(f_\alpha\rho_\mathrm{s}T_\mathrm{s}^{2.6}) \sim 10$'s of ps. Since ICF implosions are dynamic, thermodynamic instability is eventually terminated by expansion as the system blows itself apart.

Here, ignition in a fusion plasma is a statement about power balance, as it has been historically[2], and many works have generated criteria to estimate crossing this threshold in the ICF context[99–107], a context that Lawson's 1957 work only speculated about. Conceptually simpler, "gain" is a statement about energy thresholds. Since ICF has many stages of concentrating energy at successively smaller volumes, a number of definitions of gain are commonly used. Namely, target gain (or just Gain), $G_{\mathrm{target}} = Y_{\mathrm{tot}}/E_{\mathrm{las}}$ is the ratio of total fusion yield (Y_{tot}) to laser energy input to the target (E_{las}), capsule gain, $G_{\mathrm{cap}} = Y_{\mathrm{tot}}/E_{\mathrm{abs}}$, which compares the yield to capsule absorbed energy, and fuel (or DT) gain, $G_{\mathrm{fuel}} = Y_{\mathrm{tot}}/E_{\mathrm{fuel}}$, compares the yield to the energy absorbed into the DT fuel[108]. Note that $G_{target} > 1$ does not imply net energy gain from a practical fusion energy perspective because the energy consumed by the laser facility is considerably larger than E_{las}. The terms ignition and target gain have sometimes been conflated [109] for simplicity, because the impulsive nature of an implosion can complicate the assessment of the power balance near the tipping-point of ignition and the methods to do so (described below) were not developed until the past decade.

Herein gain values, G_{target}, G_{cap}, and G_{fuel} (Table I) and ignition metrics (Table II) are calculated for the NIF experiment N210808 (and database of preceding shots). The processes of alpha-heating can significantly modify hot-spot properties, as a result some ignition metrics are phrased in terms of "α-off" (aka no-α) properties [101, 102, 110], which represent the inferred plasma conditions that would be present in the implosion if alpha-heating did not occur. The value of α-off metrics lies in their ability to identify the presence of an ignition cliff whereby small incremental changes in the metric result in large shifts in fusion yield as a result of alpha-heating. In order to use no-α conditions, a model is used to translate measured properties into inferred no-α properties, which introduces a model uncertainty into the assessment. Alternatively, some ignition metrics are developed to directly use measured "α-on" properties, avoiding an intermediate model translation, but these also have uncertainty due to the feedback of alpha-heating on the plasma properties used in the metric which the underlying theory attempts to account for. In this assessment, a suite of both α-on and no-α ignition metric types are utilized based upon the data from Table I.

Based upon a definition of ignition as doubling of the hot-spot temperature due to alpha-heating, which corresponds to $Y_{\mathrm{amp}} \approx 30$, Lindl et al. [106] derive both α-on and no-α ignition metrics for one-dimensional (1D) x-ray driven ICF targets and calibrate the model to sim-
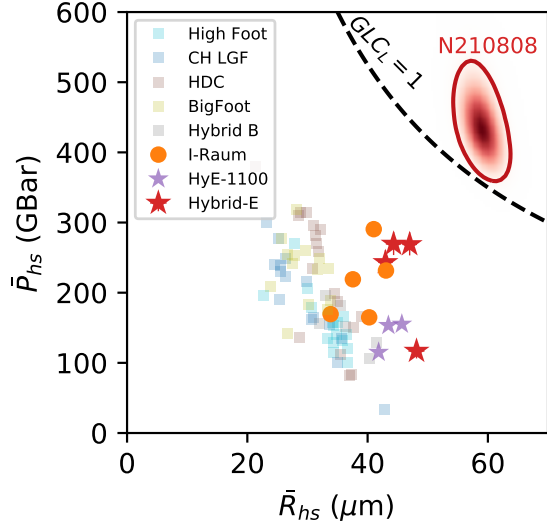
FIG. 3. NIF DT shot data (symbols) are plotted in the space of time-averaged inferred hot-spot pressure ($\bar{P}_{hs}$) and hot-spot radius ($\bar{R}_{hs}$). The black dashed curve denotes the ignition boundary from Eq. 2. Data from the Hybrid-E series is highlighted in red. DT shot N210808 is the datum in the upper-right of the plot, shown as the probability distribution from Markov Chain Monte Carlo (MCMC) analysis with a contour enclosing 80% of the distribution.

FIG. 4. NIF DT shot data (symbols) are plotted in the space of inferred Lawson parameter and hot-spot thermal temperature. The black curve denotes the ignition boundary from Eq. 3. The dotted and dashed curves show how the ignition boundary moves to higher temperature under different assumptions of mixing of high-Z material into the DT resulting in enhancement of bremsstrahlung x-ray losses (dotted: a 50% increase in bremsstrahlung, $f_B = 1.5$, and dashed: a 100% increase, $f_B = 2.0$). Data from the Hybrid-E series is highlighted in red. In this analysis, the NToF inferred DD ion temperature, $T_i(DD)$, is used as an estimate of T_{th} as previous work[111] measuring electron temperature (T_e) has shown that $T_e \approx T_i(DD) \leq T_i(DT)$ for these types of implosions.

ulations. Lindl's model emphasizes the effect of ablator remaining mass and kinetic energy on the ignition metric, and a useful α-on ignition metric, a Generalized Lawson Criterion, GLC_L, that can be compared to data-inferred quantities is obtained

$$GLC_L = \frac{\bar{P}_{\text{hs}}}{420\ Gbar} \frac{\bar{R}_{\text{hs}}}{50\ \mu m}, \qquad (2)$$

where $GLC_L > 1$ determines ignition. Lindl et al. utilizes quantities for pressure and radius that are burn-weighted in both time and space. We denote these time-averaged quantities $\bar{P}_{\text{hs}}$ and $\bar{R}_{\text{hs}}$ to distinguish them from the main inferences in this paper, which are the spatially-burn-weighted quantities at peak burn. The time-averaged pressure is inferred using the prescription in Ref. 94. The radius defined in Ref. 106 is larger than the radius determined from neutron data (i.e. Table I) and we adjust the value using relations given in Ref. 106. As shown in Fig. 3, unlike all previous shots on NIF, N210808 ignited by the definition of Eq. 2. We generate a probabilistic distribution of the GLC_L (and other metrics that follow below) using Markov Chain Monte Carlo (MCMC) analysis, following the methodology developed in Refs. 3, 94 which is used to evaluate the likelihood that $GLC_L > 1$, which is 99.6% for this criterion.

Hurricane et al. [107] frames self-heating in terms of thermodynamics, where ignition becomes a phase-change-like process that breaks the adiabaticity of the

FIG. 5. NIF DT shot data are plotted against the ignition metrics of alpha energy to hot-spot energy fraction, Eq. 4 (left) and Eq. 5 (right). The ordinate is the yield amplification (Y_{amp}). Data from the Hybrid-E series are highlighted in red. On the left, inferred quantities from both 0-D (closed symbols and red oval probability distribution) and 1-D (open symbols and purple oval probability distribution) hot-spot models are shown.

hot-spot, causing a momentary exponential jump in plasma pV^γ ($\gamma = 5/3$ being the polytropic index for DT) and a violation of Boyle's law (i.e. instead of p decreasing with V it increases, because intensive self-heating momentarily outraces expansion during the explosion-phase of an ICF implosion). The thermodynamic ignition condition (Eq. (31) of Ref. [107]) again has the form of a GLC and is not limited to 1D implosions, but more generally applies to any 3D configuration (with asymmetric modes < 6),

$$GLC_H = p_{\mathrm{hs}} \tau_{\mathrm{BW}} H(T_{\mathrm{hs}}) > 1, \qquad (3)$$

where $H(T_{\mathrm{hs}})$ is a complicated function of temperature (see Appendix on the "Thermodynamic ignition condition H-function," and Eqs. (27) and (28) of Ref. [107]) and depends upon the measure of x-ray loss enhancement due to the potential presence of high-Z mixing into the hot DT plasma, expressed by the $f_B \sim \bar{Z}^2 > 1$ of Eq. 1, with $\bar{Z}$ being the mass average atomic number. While not originally intended to correspond to a particular Y_{amp}, simulations show that $GLC_H = 1$ corresponds to a tight range of $Y_{\mathrm{amp}} \sim 16-32$ for a wide range of DT implosion types[112], consistent with the prior metrics.

Fig. 4 shows a plot of Eq. 3 with DT shot data. While Eq. 3 shows an uncertainty in the location of the ignition boundary, due to different high-Z mix assumptions, the datum for experiment N210808 is above the range of ignition boundary uncertainty. This figure shows that the conclusion of N210808 passing the ignition boundary is insensitive to uncertainties in how much material has mixed into the hot spot.

Assuming that all α energy, $E_\alpha = Y/5$, remains in the DT hot-spot, either by stopping in the hot-spot directly causing heating (the f_α stopping fraction) or by ablating the cold fuel surrounding the hot-spot $(1 - f_\alpha)$ adding mass to the hot-spot (such that $d(mT_{\mathrm{th}})/dt = 0$, an assumption that can be broken if α's are lost to pockets of cold plasma or exit the implosion via aneurisms), the parameter $E_\alpha/(2E_{\mathrm{hs}})$, where $E_{\mathrm{hs}} = c_{\mathrm{DT}} m T_{\mathrm{th}} = (3/2) p_{\mathrm{hs}} V$ is the hot-spot internal energy, provides another ignition metric [113]. Namely, by comparison to a large suite of ICF simulations and from a semi-analytic compressible shell model of the hot spot propagating into the surrounding shell, the transition to ignition has been found by Christopherson et $al.$ [113]

$$\frac{E_\alpha}{2E_{\mathrm{hs}}} > 1.4, \qquad (4)$$

where the factor of 2 in the denominator approximately accounts for the fact that only half the full yield of the implosion is generated at the time of peak burn. (Note that in Ref. [113], Eq. 4 is defined as "f_α," but that definition is not used here to avoid confusion with the α stopping-fraction in Eq. 1.) The left frame of Fig. 5 plots Eq. 4 for the suite of NIF DT shot data with

N210808 being the probability distributions to the upper right, again indicating ignition by a margin outside of the error bar of the inferred metric. Here E_{hs} is sensitive to the inference methodology; values from both 0-D and 1-D hot-spot models [94] are shown (closed and open symbols as well as red and purple distributions, respectively).

Next, the Ignition Threshold Experiment Metric ($ITFX$) gives another alternative for assessing ignition. In simulations, the product of fusion yield in the 13-15 MeV energy range (Y_{13-15}) and the square of downscatter ratio, DSR (the ratio of yield in the 10-12 MeV range over $Y_{13\text{-}15}$), correlate with Y_{amp} and ignition as found by Spears et $al.$ [30]. The most up to date version of $ITFX$ is documented by Patel et $al.$ [40]

$$ITFX_{\mathrm{no}\text{-}\alpha} = ITFX_\alpha e^{-0.9 ITFX_\alpha^{0.47} + 0.007 ITFX_\alpha^{1.65}} \quad (5)$$

where

$$ITFX_\alpha = \left(\frac{170\ \mu g}{m_{\mathrm{fuel}}}\right)\left(\frac{Y_{13\text{-}15}}{4.0 \times 10^{15}}\right)\left(\frac{DSR}{0.067}\right)^{2.1} \quad (6)$$

where m_{fuel} is the total DT fuel mass in the implosion. Eq. 5 and 6 were obtained by fitting to a large database of simulations [114]. By construction, there is a 1-1 relationship between $ITFX_{\mathrm{no}\text{-}\alpha}$ and Y_{amp}, namely $Y_{\mathrm{amp}} = \exp(0.9 ITFX_\alpha^{0.47})$ (as reflected in right frame of Fig. 5). $ITFX$ also has a simple approximate connection to the $\chi_{\mathrm{no}\text{-}\alpha}$ Lawson-like ignition metric [101, 103, 110], namely $\chi_{\mathrm{no}\text{-}\alpha} \approx ITFX_{\mathrm{no}\text{-}\alpha}^{0.34}$, making the two metrics interchangeable. As can be seen on the right frame of Fig. 5, experiment N210808 (the datum farthest to the right), passes the $ITFX$ threshold for ignition, with a likelihood of 100%.

Several ignition criteria have been developed for the conditions reached in a space of areal density (ρR) and temperature. Atzeni and Meyer-Ter-Vehn [108], Tipton[116] (most conservative case of the criteria by setting the cold fuel density term to zero), and Cheng et al. [115] have defined such criteria in terms of the hot-spot areal density (ρR_{hs}), while Coutant [117] considered total fuel areal density (ρR_{tot}). These criteria are shown in Fig. 6. In terms of hot-spot areal density, several burning-plasma shots (Ref. 3) are close to the boundary while N210808 clearly exceeds all these criteria. In terms of the ρR_{tot} criterion from Coutant et $al.$ 117, only N210808 passes the criterion. (Note some of these conditions neglect the mechanical energy loss of negative pdV work and are thus unable to distinguish between a 'burning plasma' and 'ignition.') Lastly a criterion on the second derivative of temperature ($d^2T/dt^2 > 0$) at hot spot minimum volume, which represents that the implosion is thermodynamically prepared to heat even as the hot spot expands, was suggested by Rosen and Szoke [118] then later discussed in Springer [104]; N210808 is the first shot to pass as inferred from post-shot simulations by Kritcher et $al.$ [16].

TABLE II. Likelihood of N210808 surpassing several scientific metrics developed for ignition in inertial fusion.

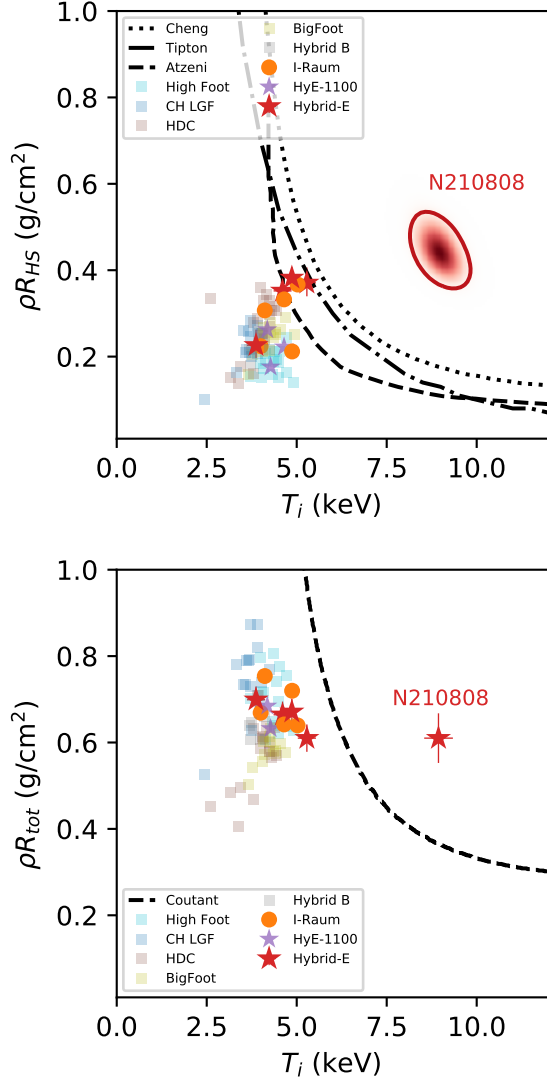|		Likelihood	
Metric	N210207	N210307	N210808
GLC_L	0%	0%	99.6%
GLC_H	0%	0%	100%
$\frac{E_\alpha}{2E_{\mathrm{hs}}}$ (0-D)	0%	0%	100%
$\frac{E_\alpha}{2E_{\mathrm{hs}}}$ (1-D)	0%	0%	99.8%
$ITFX_{no-\alpha}$	0%	0%	100%
Cheng	0%	0%	100%
Tipton	6.2%	0%	100%
Atzeni	100%	100%	100%
Coutant	0%	0%	100%
$d^2T/dt^2 > 0$	No	No	Yes
NAS 1997	No	No	No

FIG. 6. NIF DT shot data (symbols) is plotted in the space of fuel areal-density [ρR, hot-spot only (top) and total (bottom)] and hot-spot thermal temperature. The curves denote the ignition boundaries published in Cheng *et al.* [115], Tipton [116], Atzeni and Meyer-ter-Vehn [108] and Coutant [117].

We have now considered several ignition metrics, which are summarized in Table II in terms of the likelihood of shots passing the criteria. We find that N210808 passes all criteria with high likelihood, except for the $G_{\mathrm{target}} > 1$ definition of the 1997 NAS committee [109], which is not related to the physics of alpha-heating, unlike the other criterion considered in this Letter.

While experiments with $G_{\mathrm{fuel}} > 1$ have previously been reported [57, 68], N210808 is the first ICF experiment to demonstrate capsule gain ($G_{\mathrm{cap}} > 1$) achieving $G_{\mathrm{cap}} \sim 5.8$. The overall target gain is $G_{\mathrm{target}} \sim 0.72$, which is substantially larger than any prior ICF experiment, the highest of which (N210207) was ~ 0.09 (Ref. [3], see

Table I). That relatively modest changes were made to "burning plasma" experiments [3, 4] to obtain the results in Experiment N210808 emphasizes the sensitivity of ICF implosions near the ignition threshold. The fact that the DT plasma properties themselves jumped to significantly higher values, as reflected in the large change of p_{hs}, T_{th}, V, E_{hs}, Y_{total}, and G's, is in itself a qualitative indication of ignition.

Efficient fusion fuel burn-up requires the fusion rate per unit mass $Q_\alpha \sim \rho T_{th}^n$ be as large as possible over the confinement time. Here n is well approximated by $7/T_{th}^{0.2}$, a decreasing function of T_{th} (in keV), with a local power law exponent sensitivity $7(1 - 0.2\log(T_{th}))/T_{th}^{0.2} = 3.4$ (2.4) for a 5 (10) keV Maxwellian distribution [119]. The gain of the system is ultimately limited by the fraction of fuel that can be "burned," during a confinement time set by hydrodynamic expansion ($\sim R_{hs}/v$ where the expansion speed $v \sim \sqrt{T_{th}}$) which scales as the measurable product $\rho R T_{th}^{n-0.5}$ [106]. Previous implosions have been limited to < 0.3 % burn-up fraction [3] whereas this work reached 1.9%. Even the most maximally efficient ICF burn-up fractions are realistically limited to levels of a couple $\sim 10's$%, because the regime of strong propagating burn is truncated by explosion, rather than hot spot conduction and radiation losses.

In summary, the August 8, 2021 experiment on the National Ignition Facility is the first time that Lawson's ignition criterion was unambiguously achieved in the laboratory. This demonstrates that the ignition threshold is real, largely consistent with theoretical expectations, and that a laboratory or reactor-scale plasma can be ignited. However, the demonstrated level of target gain on N210808, and the underlying scheme of x-ray driven implosions is not *yet* practical for fusion energy applications. Near repeat implosions since N210808 have reached 1/3 to 1/2 of the 1.3 MJ yield and correspond-

ing lower T_{ion}, consistent with not having yet reached the expected performance plateau (i.e. not yet having "margin") at the current areal density [106]. Attaining more robust and eventually higher yields have motivated plans to increase the areal density by scale and/or ablator/fuel thickness while maintaining similar v_{imp} and coast time. This in turn will require further improving the hohlraum efficiency (e.g. smaller LEHs, interior LEH shields [120, 121], lower surface area to volume frustum-shaped "Frustraum" hohlraums [122]) and/or increasing NIF energy [123]. Further research tracks are aimed at improving compression of HDC and hence maximum attainable density and yield [124] by modifying laser pulse and dopant profile [125], using thicker ablators, revisiting high compression CH or other amorphous ablator designs in low gas-fill hohlraums with symmetry control by beam staggering [126] and adding magnetically assisted confinement [127]. Additionally, future studies will assess the impact of potentially non-Maxwellian distributions of D and T ions inferred from nuclear time-of-flight spectra [128].

(deceased), R. Kidder (deceased), R. C. Kirkpatrick, C. Max, W. Mead, S. Obenschain, D. Phillion, D. Shvarts, M. Sluyter, H. D. Shay, R. Thiessen, and L. Wood.

[†]Deceased

Appendix on the History of ICF experiments on the NIF – After developing on or adapting ICF instrumentation [129] and techniques [13] to the NIF to measure, and by adjusting laser and target parameters, control the peak drive [130, 131], drive temporal profile [14, 132], capsule trajectory [74] and symmetry [133–135], the 192 beam layered implosions began with intentionally dudded THD (tritium-hydrogen-deuterium) implosions [136, 137]. The NIF commenced layered DT experiments in June 2011 with the "low-foot" design [15] that used a 4-shock drive in a high gas-fill (i.e. 0.96 mg/cm^3 He) hohlraum to create a low entropy, hence high $30-35\times$ convergence ratio (initial radius/stagnation radius), implosion using nominally 0.93 mm inner radius mid-Z doped CH polymer capsule ablators [138]. The hohlraum gas fill density was chosen to impede the hohlraum wall plasma expansion and maintain drive symmetry over the time duration required for the 20 ns low entropy pulse shapes. The 2011-2012 experiments [139, 140] that reached 2.5 kJ yield were impacted by significant time-dependent laser-plasma instability (LPI) losses primarily on the inner cone [141] leading to undesirable implosion asymmetry swings [29, 142–144] exacerbated by having to use fixed wavelength detuning between beam cones to promote cross beam energy transfer (CBET) to the inner cone by 3-wave mixing [145]. They were also impacted by hydrodynamic instabilities [146–148] more than expected, as later proven by a brief "adiabat-shaping" series that raised the picket energy (first ~ 1 ns) of the pulse [149] to reduce the ablation front instability [150] leading to a $\sim 3\times$ increase in yield while maintaining relatively high compression [151].

A 3-shock "high-foot" design [28, 55] applies a stronger first shock by raising the laser power, thus hohlraum radiation temperature, in the "foot" (the time duration of the laser-pulse before the rise to peak power, see Fig. 1b). The modification improves hydrodynamic stability [152] during first shock passage [153], but also increasing DT fuel entropy and reducing compression. The 3-shock high foot accessed higher T_{ion} and higher fusion yield [56] ultimately reaching 25 kJ [154], but asymmetry and the re-emergence of instability capped performance as $v_{imp} \sim 390$ km/s was approached [155, 156]. High-foot designs used the same targets as the low-foot design but with a higher (1.6 mg/cm^3) gas fill, consequently it suffered from similar hohlraum problems (high LPI and poor symmetry control). During the high-foot series of experiments, it was first seen that reducing peak laser power while extending the duration of peak laser power, thus reducing "coast time" (herein quantitatively defined as mid fall of the laser power at the end of the pulse to time of peak compression, see Fig. 1b), led to a significant simultaneous increase in implosion compression and fusion yield [157] and thus to the first indications of alpha-particle self-heating [57, 158], albeit the physics behind the increase was speculative at the time.

Parallel efforts exploring so-called "exploding pushers" for neutron diagnostic flat-fielding [59, 159] and traditional ablative designs [58, 160] in near vacuum hohlraums mitigated losses due to LPI leading to a transition away from high gas-fill to low gas-fill hohlraums [161–163]. However, without a high gas-fill, the ratio of hohlraum to capsule diameter needed to be larger for long pulse CH designs [164] to delay the ingress of hohlraum plasma into the path of the inner laser beams [165], reducing coupling efficiency from hohlraum to capsule. An alternate strategy reduced the pulse length by equalizing the picket and trough power at the expense of greater classical ablation front growth, applicable to Be ablator designs that compensate by more ablative stabilization of that growth [166].

To mitigate the lower energy coupling and poor symmetry control of CH ablators in high gas fill hohlraums, implosions using high density carbon (HDC) ablators were investigated. HDC ablators [167] doped with W for x-ray preheat shielding [168], which are relatively thinner than CH (for fixed capsule mass because of the density difference of 3.3-3.5 g/cm^3 for HDC vs. 1.05 g/cm^3 for CH and 1.85 g/cm^3 for Be), allowed for shorter laser pulses [169, 170] and hence lower hohlraum He gas-fill

(0.3 mg/^{3}) while maintaining acceptable hohlraum wall ingress [66]. With lower gas pressures and shorter pulses, the energy lost to backscattered light was significantly reduced, increasing the overall coupling efficiency from 80% to 98%. Additionally, symmetry could be controlled without the need for CBET. Two-shock "BigFoot" [171–173] and 3-shock "HDC" designs [174, 175] of implosion were inherently even higher entropy and lower convergence due to the requirement to melt the crystalline HDC with a sufficiently strong first shock passage to avoid seeding instability growth at the ablator-fuel interface [169, 176, 177]. Such implosions reached 55 kJ of yield for similar capsule inside radius as earlier CH designs and seemed to be less affected by the hydrodynamic perturbations from the tent membrane (typically a 45 nm thick formvar film that holds the capsule in the center of the hohlraum, see Fig. 1a) as predicted by high resolution capsule simulations [178], but were more susceptible to hydrodynamic perturbations from the fill tube and hole. Analysis of the experiments [51, 179] and simulations [180] motivated an engineering effort to reduce the fill tube diameter. Three dimensional (3D) simulations performed with HYDRA suggest that MJ yields could not be obtained [181] even if all degradations were removed from this initial HDC design. Theory and simulations indicated greater performance could be obtained with a larger capsule that absorbed more energy.

In parallel, experimentally observed limits [60] on convergence levels with HDC based ablators along with theory scalings based upon existing implosion data [61] motivated an alternate "HYBRID" (high yield big radius implosion design) strategy using larger capsules [62, 63] to increase energy coupled to the hot spot without sacrificing stagnation pressure. Thus, in the "HYBRID-B" design, the capsule radius was increased by up to 20%, but the shell areal density was only increased in by 10% in order to maintain high v_{imp} [182]. While the design was developed to eventually use 2.05 MJ of laser energy, implosions using the 1.9 MJ laser input available showed the expected improvement in yield for a given v_{imp} by increasing scale [182]. These implosions also showed bright x-ray emission features [41] which correlated with reduced yield and an increase in imperfections in manufacturing larger capsules (voids in the bulk and pits on the surface), defects that remain an engineering challenge even today. Meanwhile, numerical modeling combined with data-driven models [66] for hohlraum wall motion dynamics [183–185], and for CBET developed for low gas-filled hohlraums [67] improved drive symmetry understanding and control. This enabled shrinking the hohlraum size by 5% for $\sim$ 10% gain in efficiency while maintaining adequate drive symmetry in the "HYBRID-E" [54] and spool shaped "I-Raum" [186] designs. Fusion output on HYBRID-E and I-Raum designs reached 170 kJ and entered the burning plasma regime [3, 4, 53, 187].

Appendix on Laser improvements – Laser pulse shaping and master oscillator design changes were implemented earlier in 2020 and 2021 to improve power accuracy and balance of NIF's 192 beams in the hohlraum, contributing to improved implosion control and symmetry. Better control of the picket power accuracy and peak of the pulse was achieved by updating the NIF laser master oscillator room (MOR) with currently available fiber optic modulation and amplification technologies and reducing amplifier gain uncertainty in the NIF 4-pass preamplifiers. The newly deployed MOR architecture demonstrated a $2 - 3\times$ shot-to-shot stability improvements of the pulse train before shaping and a mitigation of the power droop at the peak of ignition pulses [188]. Shot-to-shot gain stability of the pre-amplifier module employing a 32 mm diameter flashlamp-pumped LHG-8 Nd:glass rod amplifier improved from 5% rms to better than 3% rms.

Appendix on Thermodynamic ignition condition H-function: The function $H(T)$ in Eq. 3 is (see Fig. 7)

$$H(T) = \frac{\sqrt{\pi}F(T)}{\sqrt{\frac{2\gamma}{\gamma-1} + \frac{2T}{F(T)}\frac{\partial F}{\partial T}}}. \tag{7}$$

where $\gamma = 5/3$ is the polytropic index and the function $F(T)$ is a measure of the competition between alpha-heating and bremsstrahlung cooling evaluated at peak hotspot pressure.

$$F(T) = \frac{3}{2}\frac{Q_\alpha - f_B Q_B}{\rho(c_{DT}T)^2} \tag{8}$$

The parameter f_B reflects the DT bremsstrahlung enhancement at peak hotspot pressure. Note that $F = 0$ at the "ignition temperature" $T_{ign} = 4.3f_B^{0.3}$ in keV.

---

* hurricane1@llnl.gov
[1] R. F. Post, Rev. Mod. Phys. **28**, 338 (1956).
[2] J. D. Lawson, Proceedings of the Physical Society. Section B **70**, 6 (1957).
[3] A. Zylstra, O. Hurricane, *et al.*, Nature **601**, 542 (2022), https://doi.org/10.1038/s41586-021-04281-w.
[4] A. Kritcher, C. Young, H. Robey, *et al.*, Nature Physics (2022), 10.1038/s41567-021-01485-9, https://doi.org/10.1038/s41567-021-01485-9.
[5] E. I. Moses *et al.*, Journal of Physics: Conference Series **688**, 012073 (2016).
[6] B. J. Green, I. I. Team, and P. Teams, Plasma Physics and Controlled Fusion **45**, 687 (2003).
[7] J. Nuckolls, L. Wood, A. Thiessen, and G. Zimmerman, Nature **239**, 139 (1972).
[8] J. S. Clarke, H. N. Fisher, and R. J. Mason, Phys. Rev. Lett. **30**, 249 (1973).
[9] C. B. Tarter, *The American Lab* (Johns Hopkins University Press, Baltimore, Maryland, 2018) pp. 153–172.
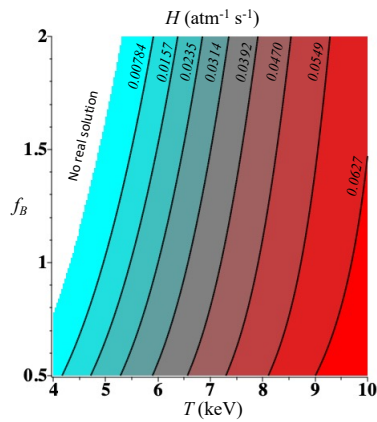[10] J. Lindl, Phys. Plasmas **2**, 3933 (1995).

FIG. 7. The contour plot of H shows the dependence upon f_B and T. At fixed T, higher f_B lowers H essentially reflecting the fact that enhanced bremsstrahlung cooling makes the ignition temperature higher than it would be for pure DT and this makes ignition more difficult to achieve. If the implosion can be engineered to have a high enough optical depth to reabsorb bremsstrahlung x-rays ($f_B < 1$), the ignition temperature is reduced.

[11] G. Guderley, Luftfahrtforshung **19** (1942).
[12] O. L. Landen *et al.*, Phys. Plasmas **17**, 056301 (2010).
[13] O. L. Landen *et al.*, Phys. Plasmas **18**, 051002 (2011).
[14] H. F. Robey *et al.*, Phys. Rev. Lett. **108**, 215004 (2012).
[15] S. W. Haan *et al.*, Phys. Plasmas **18** (2011).
[16] A. L. Kritcher *et al.*, Phys. Rev. E **XX**, XXXXXX (2022).
[17] J. Moody *et al.*, Phys. Plasmas **24**, 042709 (2017).
[18] O. A. Hurricane *et al.*, Phys. Plasmas **24**, 092706 (2017).
[19] O. A. Hurricane *et al.*, Physics of Plasmas **29**, 012703 (2022), https://doi.org/10.1063/5.0067699.
[20] P. Volegov *et al.*, Rev. Sci. Instrum. **85**, 023508 (2014).
[21] G. S. Fraley, E. J. Linnebur, R. J. Mason, and R. L. Morse, The Physics of Fluids **17**, 474 (1974), https://aip.scitation.org/doi/pdf/10.1063/1.1694739.
[22] C. Haynam, P. Wegner, J. Auerbach, *et al.*, Applied Optics **46**, 3276 (2007).
[23] M. L. Spaeth, K. R. Manes, D. H. Kalantar, *et al.*, Fusion Science and Technology **69**, 25 (2016), https://doi.org/10.13182/FST15-144.
[24] B. M. V. Wonterghem, R. L. Kauffman, D. W. Larson, and M. C. Herrmann, Journal of Physics: Conference Series **717**, 012085 (2016).
[25] M. D. Rosen, Phys. Plasmas **6**, 1690 (1999), https://doi.org/10.1063/1.873427.
[26] J. D. Lindl *et al.*, Phys. Plasmas **11**, 339 (2004).
[27] M. C. Herrmann, M. Tabak, and J. D. Lindl, Nuclear Fusion **41**, 99 (2001).
[28] T. R. Dittrich *et al.*, Phys. Rev. Lett. **112** (2014).
[29] A. L. Kritcher *et al.*, Phys. Plasmas **21** (2014).
[30] B. K. Spears *et al.*, Phys. Plasmas **21**, 042702 (2014).
[31] O. A. Hurricane *et al.*, Phys. Plasmas **27**, 062704 (2020).
[32] B. J. MacGowan *et al.*, High Energy Density Physics **40**, 100944 (2021).
[33] C. V. Young, L. Masse, D. T. Casey, *et al.*, Physics of Plasmas **27**, 082702 (2020).
[34] D. T. Casey *et al.*, Phys. Rev. Lett. **126**, 025002 (2021).

[35] B. A. Hammel, S. W. Haan, D. S. Clark, *et al.*, Physical Review Letters **6**, 171 (2010).
[36] D. S. Clark, S. W. Haan, A. W. Cook, *et al.*, Phys. Plasmas **18**, 082701 (2011), https://doi.org/10.1063/1.3609834.
[37] V. Smalyuk, C. Weber, O. Landen, *et al.*, High Energy Density Physics **36**, 100820 (2020).
[38] S. P. Regan, R. Epstein, B. A. Hammel, *et al.*, Phys. Rev. Lett. **111**, 045001 (2013).
[39] T. Ma *et al.*, Phys. Rev. Lett. **111**, 085004 (2013).
[40] P. K. Patel *et al.*, Phys. Plasmas **27**, 050901 (2020).
[41] A. B. Zylstra, D. T. Casey, A. Kritcher, *et al.*, Phys. Plasmas **27**, 092709 (2020), https://doi.org/10.1063/5.0003779.
[42] S. R. Nagel, S. W. Haan, J. R. Rygg, *et al.*, Phys. Plasmas **22**, 022704 (2015), https://doi.org/10.1063/1.4907179.
[43] R. Tommasini, J. E. Field, B. A. Hammel, *et al.*, Phys. Plasmas **22** (2015), 10.1063/1.4921218, 56th Annual Meeting of the APS Division of Plasma Physics, New Orleans, LA, OCT 27-31, 2014.
[44] J. E. Ralph, T. Döppner, D. E. Hinkel, *et al.*, Phys. Plasmas **27**, 102708 (2020), https://doi.org/10.1063/5.0017931.
[45] A. MacPhee, D. Casey, D. Clark, *et al.*, Physical Review E **95**, 031204(R) (2017).
[46] A. MacPhee, D. Casey, D. Clark, *et al.*, Physical review. E **95** (2017), 10.1103/PhysRevE.95.069905.
[47] D. A. Martinez, V. A. Smalyuk, A. G. MacPhee, *et al.*, Physics of Plasmas **24** (2017), 10.1063/1.4995568.
[48] C. R. Weber, D. T. Casey, D. S. Clark, *et al.*, Physics of Plasmas **24** (2017), 10.1063/1.4977536.
[49] A. G. MacPhee, V. A. Smalyuk, O. L. Landen, *et al.*, Phys. Plasmas **25** (2018), 10.1063/1.5025183.
[50] M. A. Barrios, S. P. Regan, L. J. Suter, *et al.*, Physics of Plasmas **20** (2013), 10.1063/1.4816034.
[51] A. Pak *et al.*, Phys. Rev. Lett. **124**, 145001 (2020).
[52] B. Bachmann, J. E. Ralph, A. B. Zylstra, *et al.*, Phys Rev E **101**, 033205 (2020).
[53] A. B. Zylstra *et al.*, Phys. Rev. Lett. **126**, 025001 (2021).
[54] A. L. Kritcher *et al.*, Phys. Plasmas **28**, 072706 (2021).
[55] D. H. Hinkel *et al.*, Plasma Phys. Control. Fusion **55**, 124015 (2013).
[56] H.-S. Park *et al.*, PHYSICAL REVIEW LETTERS **112** (2014), 10.1103/PhysRevLett.112.055001.
[57] O. A. Hurricane *et al.*, Nature **506**, 343 (2014).
[58] S. Le Pape *et al.*, Phys. Plasmas **23** (2016), 10.1063/1.4950843, 57th Annual Meeting of the APS-Division-of-Plasma-Physics (DPP), Savannath, GA, NOV 16-20, 2015.
[59] L. Divol *et al.*, Phys. Plasmas **24** (2017), 10.1063/1.4982215, 58th Annual Meeting of the APS-Division-of-Plasma-Physics (DPP), San Jose, CA, OCT 31-NOV 04, 2016.
[60] O. L. Landen *et al.*, Phys. Plasmas **28**, 042705 (2021), https://doi.org/10.1063/5.0033256.
[61] O. A. Hurricane, D. A. Callahan, M. J. Edwards, *et al.*, 59th Annual Meeting of the American Physical Society Division of Plasma Physics (vol. 62, no. 12, abstract PO7.00001), Milwaukee, WI Oct. 23-27, unpublished (2017).
[62] O. A. Hurricane *et al.*, Plasma Phys. Control. Fusion **61** (2019).
[63] O. A. Hurricane *et al.*, Phys. Plasmas **26**, 052704 (2019).

[64] M. Hohenberger *et al.*, Phys. Plasmas **27**, 112704 (2020), https://doi.org/10.1063/5.0019083.

[65] A. B. Zylstra *et al.*, Phys. Plasmas **27**, 092709 (2020), https://doi.org/10.1063/5.0003779.

[66] D. A. Callahan *et al.*, Phys. Plasmas **25** (2018).

[67] A. L. Kritcher *et al.*, Phys. Rev. E **98**, 053206 (2018).

[68] S. Le Pape *et al.*, Phys. Rev. Lett. **120**, 245003 (2018).

[69] L. B. Hopkins *et al.*, PLASMA PHYSICS AND CONTROLLED FUSION (2018).

[70] K. L. Baker *et al.*, Phys. Rev. E **102**, 023210 (2020).

[71] A. Zylstra *et al.*, Nucl. Fusion **61**, 116066 (2021).

[72] J. E. Ralph *et al.*, 63rd Annual Meeting of the American Physical Society Division of Plasma Physics (vol. 66, no. 13, abstract GO04.00003), Pittsburgh, PA, Nov. 8-12, unpublished (2021).

[73] A. B. Zylstra *et al.*, Phys. Rev. E **XX**, XXXXXX (2022).

[74] D. G. Hicks, N. B. Meezan, E. L. Dewald, *et al.*, Physics of Plasmas **19** (2012), 10.1063/1.4769268.

[75] V. Smalyuk, L. Atherton, L. Benedetti, *et al.*, Physical Review Letters **111** (2013), 10.1103/PhysRevLett.111.215001.

[76] A. B. Zylstra *et al.*, Phys. Plasmas **21**, 112701 (2014).

[77] M. M. Marinak *et al.*, Phys. Plasmas **8**, 2275 (2001), https://doi.org/10.1063/1.1356740.

[78] L. X. Benedict *et al.*, Phys. Rev. B **89**, 224109 (2014).

[79] J. Gaffney *et al.*, High Energy Density Physics **28**, 7 (2018).

[80] M. P. Desjarlais, C. R. Scullard, L. X. Benedict, H. D. Whitley, and R. Redmer, Phys. Rev. E **95**, 033203 (2017).

[81] L. G. Stanton and M. S. Murillo, Phys. Rev. E **93**, 043203 (2016).

[82] Y. T. Lee and R. M. More, The Physics of Fluids **27**, 1273 (1984), https://aip.scitation.org/doi/pdf/10.1063/1.864744.

[83] C. R. Scullard, S. Serna, L. X. Benedict, C. L. Ellison, and F. R. Graziani, Phys. Rev. E **97**, 013205 (2018).

[84] C. A. Iglesias and F. J. Rogers, Astrophys. J. **464**, 943 (1996).

[85] J. L. Milovich, D. C. Casey, B. MacGowan, *et al.*, PLASMA PHYSICS AND CONTROLLED FUSION **63**, 025012 (2021).

[86] D. A. Callahan *et al.*, Phys. Plasmas **27**, 072704 (2020), https://doi.org/10.1063/5.0006217.

[87] D. L. Bleuel *et al.*, Rev. Sci. Instrum. **83**, 10D313 (2012).

[88] M. G. Johnson *et al.*, Rev. Sci. Instrum. **83**, 10D308 (2012).

[89] J. Frenje *et al.*, Nuclear Fusion **53**, 043014 (2013).

[90] V. Y. Glebov *et al.*, Rev. Sci. Instrum. **81**, 10D325 (2010).

[91] R. Hatarik *et al.*, J. Appl. Phys. **118**, 184502 (2015).

[92] L. Ballabio, J. Källne, and G. Gorini, Nucl. Fusion **38**, 1723 (1998).

[93] H. W. Herrmann *et al.*, Rev. Sci. Instrum. **81**, 10D333 (2010).

[94] A. Zylstra *et al.*, Phys. Plasmas **28**, 122703 (2021).

[95] Note that in ICF, and fusion in general, the fusion plasma is not in thermal equilibrium with the radiation field since the photon mean-free path is very long compared to the size of the plasma, so the blackbody energy ($4\sigma T^4/c$ with σ being the Stefan-Boltzmann constant and c being the speed of light) is not included in the heat-capacity.

[96] S. P. Lyon and J. D. Johnson, *Sesame: The Los Alamos National Laboratory Equation of State Database*, Tech. Rep. LA-UR-92-3407 (Los Alamos National Laboratory, 1995).

[97] L. Spitzer and R. Härm, Phys. Rev. **89**, 977 (1953).

[98] A. B. Zylstra and O. A. Hurricane, Phys. Plasmas **26**, 062701 (2019).

[99] R. Betti *et al.*, Phys. Plasmas **9**, 2277 (2002).

[100] C. D. Zhou and R. Betti, Phys. Plasmas **16**, 079905 (2009).

[101] P. Y. Chang *et al.*, Phys. Rev. Lett. **104** (2010).

[102] R. Betti *et al.*, Phys. Plasmas **17** (2010).

[103] R. Betti *et al.*, Phys. Rev. Lett. **114**, 255003 (2015).

[104] P. Springer *et al.*, Nucl. Fusion **59**, 032009 (2018).

[105] A. R. Christopherson *et al.*, Phys. Plasmas **25**, 012703 (2018).

[106] J. D. Lindl *et al.*, Phys. Plasmas **25**, 122704 (2018).

[107] O. A. Hurricane *et al.*, Phys. Plasmas **28**, 022704 (2021).

[108] S. Atzeni and J. Meyer-Ter-Vehn, *The Physics of Inertial Fusion* (Oxford University Press, Oxford, Great Britain, 2004) p. 120.

[109] S. Koonin *et al.*, *Review of the Department of Energy's Inertial Confinement Fusion Program: The National Ignition Facility (1997)* (National Academies Press, Washington, D.C., 1997) p. 64.

[110] C. D. Zhou and R. Betti, Phys. Plasmas **15**, 102707 (2008).

[111] L. C. Jarrott *et al.*, Phys. Rev. Lett. **121**, 085001 (2018).

[112] S. A. MacLaren *et al.*, Physics of Plasmas **28**, 122710 (2021), https://doi.org/10.1063/5.0064971.

[113] A. R. Christopherson *et al.*, Phys. Plasmas **27**, 052708 (2020).

[114] J. A. Gaffney *et al.*, Phys. Plasmas **26**, 082704 (2019).

[115] B. Cheng, P. A. Bradley, S. M. Finnegan, and C. A. Thomas, Nuclear Fusion **61**, 096010 (2021).

[116] R. Tipton, LLNL-TR-676592 (2015).

[117] J. Coutant, *La fusion thermonucléaire inertielle par laser*, edited by R. Dautray and J.-P. Watteau (Eyrolles, Paris, France, 1993) p. 30.

[118] M. Rosen and A. Szoke, Private Communication (2015).

[119] H.-S. Bosch and G. Hale, Nuclear Fusion **32**, 611 (1992).

[120] P. Amendt, S. Glendinning, B. Hammel, *et al.*, Physics of Plasmas **4** (1997), 10.1063/1.872329.

[121] D. Callahan, P. Amendt, E. Dewald, *et al.*, Physics of Plasmas **13** (2006), 10.1063/1.2196287.

[122] P. Amendt, D. Ho, Y. Ping, *et al.*, Phys. Plasmas **26**, 082707 (2019), https://doi.org/10.1063/1.5099934.

[123] J. M. D. Nicola, T. Bond, M. Bowers, *et al.*, Nuclear Fusion **59**, 32004 (2018).

[124] D. D. Ho, S. W. Haan, J. D. Salmonson, *et al.*, Journal of Physics: Conference Series **717** (2016), 10.1088/1742-6596/717/1/012023.

[125] D. S. Clark, D. T. Casey, C. R. Weber, *et al.*, Physics of Plasmas **29** (2022), 10.1063/5.0087052.

[126] R. E. Turner, P. Amendt, O. L. Landen, *et al.*, Physics of Plasmas **7**, 333 (2000).

[127] J. D. Moody, B. B. Pollock, H. Sio, *et al.*, Journal of Fusion Energy **41** (2022), 10.1007/s10894-022-00319-7.

[128] E. Hartouni *et al.*, Nature (2022), in preparation.

[129] J. D. Kilkenny, P. M. Bell, D. K. Bradley, *et al.*, Fusion Science and Technology **69**, 420 (2016).

[130] R. P. J. Town, M. D. Rosen, P. A. Michel, *et al.*, Phys. Plasmas **18**, 056302 (2011), https://doi.org/10.1063/1.3562552.

[131] J. L. Kline, D. A. Callahan, S. H. Glenzer, *et al.*, Phys. Plasmas **20**, 056314 (2013), https://doi.org/10.1063/1.4803907.

[132] D. H. Munro, P. M. Celliers, G. W. Collins, *et al.*, Physics of Plasmas **8**, 2245 (2001).

[133] G. A. Kyrala, J. L. Kline, S. Dixit, *et al.*, Phys. Plasmas **18**, 056307 (2011), https://doi.org/10.1063/1.3574504.

[134] E. L. Dewald, J. L. Milovich, P. Michel, *et al.*, Phys Rev Lett **111**, 235001 (2013).

[135] J. R. Rygg, O. S. Jones, J. E. Field, *et al.*, Phys. Rev. Lett. **112**, 195001 (2014).

[136] M. J. Edwards, J. D. Lindl, B. K. Spears, *et al.*, Physics of Plasmas **18** (2011), 10.1063/1.3592173.

[137] S. Glenzer, B. Spears, M. Edwards, *et al.*, Plasma Physics and Controlled Fusion **54** (2012), 10.1088/0741-3335/54/4/045013.

[138] A. Nikroo, K. C. Chen, M. L. Hoppe, *et al.*, Physics of Plasmas **13** (2006), 10.1063/1.2179054.

[139] M. J. Edwards, P. K. Patel, J. D. Lindl, *et al.*, Physics of Plasmas **20** (2013), 10.1063/1.4816115.

[140] J. D. Lindl *et al.*, Phys. Plasmas **21** (2014), 10.1063/1.4903459.

[141] J. Moody, D. Callahan, D. Hinkel, *et al.*, Physics of Plasmas **21** (2014), 10.1063/1.4876966.

[142] R. P. J. Town, D. K. Bradley, A. Kritcher, *et al.*, Phys. Plasmas **21**, 056313 (2014), https://doi.org/10.1063/1.4876609.

[143] A. B. Zylstra, J. A. Frenje, F. H. Seguin, *et al.*, Phys. Plasmas **22** (2015), 10.1063/1.4918355, 56th Annual Meeting of the APS Division of Plasma Physics, New Orleans, LA, OCT 27-31, 2014.

[144] A. Pak, L. Divol, A. L. Kritcher, *et al.*, Phys. Plasmas **24** (2017), 10.1063/1.4979192, 58th Annual Meeting of the APS-Division-of-Plasma-Physics (DPP), San Jose, CA, OCT 31-NOV 04, 2016.

[145] P. Michel, L. Divol, E. A. Williams, *et al.*, Phys. Rev. Lett. **102**, 025004 (2009).

[146] V. A. Smalyuk, D. T. Casey, D. S. Clark, *et al.*, PHYSICAL REVIEW LETTERS **112** (2014), 10.1103/PhysRevLett.112.185003.

[147] K. S. Raman, V. A. Smalyuk, D. T. Casey, *et al.*, Phys. Plasmas **21** (2014), 10.1063/1.4890570.

[148] V. Smalyuk, S. Weber, D. Casey, *et al.*, Physics of Plasmas **22** (2015), 10.1063/1.4926591.

[149] J. L. Milovich, H. F. Robey, D. S. Clark, *et al.*, Phys. Plasmas **22**, 122702 (2015), https://doi.org/10.1063/1.4935922.

[150] A. G. MacPhee, J. L. Peterson, D. T. Casey, *et al.*, Physics of Plasmas **22** (2015), 10.1063/1.4928909.

[151] D. T. Casey, J. L. Milovich, V. A. Smalyuk, *et al.*, PHYSICAL REVIEW LETTERS **115** (2015), 10.1103/PhysRevLett.115.105001.

[152] D. S. Clark, C. R. Weber, J. L. Milovich, *et al.*, Phys. Plasmas **23** (2016), 10.1063/1.4943527, 57th Annual Meeting of the APS-Division-of-Plasma-Physics (DPP), Savannath, GA, NOV 16-20, 2015.

[153] J. L. Peterson, D. T. Casey, O. A. Hurricane, *et al.*, Phys. Plasmas **22** (2015), 10.1063/1.4920952, 56th Annual Meeting of the APS Division of Plasma Physics, New Orleans, LA, OCT 27-31, 2014.

[154] T. Döppner, D. A. Callahan, O. A. Hurricane, *et al.*, PHYSICAL REVIEW LETTERS **115** (2015), 10.1103/PhysRevLett.115.055001.

[155] T. Ma, O. A. Hurricane, D. A. Callahan, *et al.*, PHYS-ICAL REVIEW LETTERS **114** (2015), 10.1103/PhysRevLett.114.145004.

[156] D. A. Callahan, O. A. Hurricane, D. E. Hinkel, *et al.*, Phys. Plasmas **22** (2015), 10.1063/1.4921144, 56th Annual Meeting of the APS Division of Plasma Physics, New Orleans, LA, OCT 27-31, 2014.

[157] O. A. Hurricane, D. A. Callahan, D. T. Casey, *et al.*, Phys. Plasmas **21** (2014), 10.1063/1.4874330, 55th Annual Meeting of the APS Division ofPlasma Physics, Denver, CO, NOV 11-14, 2013.

[158] O. A. Hurricane *et al.*, Nature Physics **12**, 800 (2016).

[159] S. Le Pape, L. Divol, L. Berzak Hopkins, *et al.*, Phys. Rev. Lett. **112**, 225002 (2014).

[160] S. A. MacLaren, L. P. Masse, C. E. Czajka, *et al.*, Physics of Plasmas **25** (2018), 10.1063/1.5017976.

[161] D. E. Hinkel, L. F. B. Hopkins, *et al.*, PHYSI-CAL REVIEW LETTERS **117** (2016), 10.1103/PhysRevLett.117.225002.

[162] O. S. Jones, L. J. Suter, H. A. Scott, *et al.*, Physics of Plasmas **24**, 056312 (2017).

[163] G. N. Hall *et al.*, Phys. Plasmas **24** (2017), 10.1063/1.4983142.

[164] T. Döppner, D. E. Hinkel, L. C. Jarrott, *et al.*, Phys. Plasmas **27**, 042701 (2020), https://doi.org/10.1063/1.5135921.

[165] M. B. Schneider, S. A. Maclaren, K. Widmann, *et al.*, Journal of Physics: Conference Series **717**, 5 (2016).

[166] A. Zylstra, J. Ralph, S. MacLaren, *et al.*, High Energy Density Physics **34**, 100747 (2020).

[167] J. Biener, D. Ho, C. Wild, *et al.*, Nuclear Fusion **49**, 112001 (2009).

[168] L. F. Berzak Hopkins, S. Le Pape, L. Divol, *et al.*, Phys. Plasmas **22**, 056318 (2015), https://aip.scitation.org/doi/pdf/10.1063/1.4921151.

[169] A. J. MacKinnon, N. B. Meezan, J. S. Ross, *et al.*, Phys. Plasmas **21**, 056318 (2014), https://doi.org/10.1063/1.4876611.

[170] J. S. Ross, D. Ho, J. Milovich, T. Döppner, *et al.*, Physical Review E **91**, 1 (2015).

[171] D. T. Casey, C. A. Thomas, K. L. Baker, *et al.*, Phys. Plasmas **25** (2018), 10.1063/1.5019741.

[172] K. L. Baker, C. A. Thomas, D. T. Casey, *et al.*, PHYS-ICAL REVIEW LETTERS **121** (2018), 10.1103/PhysRevLett.121.135001.

[173] K. L. Baker, C. A. Thomas, D. T. Casey, *et al.*, Phys. Rev. E **102**, 023210 (2020).

[174] S. Le Pape, L. F. Berzak Hopkins, L. Divol, *et al.*, PHYSICAL REVIEW LETTERS **120** (2018), 10.1103/PhysRevLett.120.245003.

[175] L. Berzak Hopkins, L. Divol, C. Weber, *et al.*, Phys. Plasmas **25**, 080706 (2018), https://doi.org/10.1063/1.5033459.

[176] P. M. Celliers, D. J. Erskine, C. M. Sorce, D. G. Braun, O. L. Landen, and G. W. Collins, Rev. Sci. Instrum. **81**, 035101 (2010), https://doi.org/10.1063/1.3310076.

[177] S. Ali, P. Celliers, S. Haan, *et al.*, Physics of Plasmas **25**, 092708 (2018).

[178] D. S. Clark, A. L. Kritcher, S. A. Yi, *et al.*, Physics of Plasmas **25** (2018), 10.1063/1.5016874.

[179] K. L. Baker, C. A. Thomas, T. R. Dittrich, *et al.*, PHYSICS OF PLASMAS **27**, 112706 (2020).

[180] C. R. Weber *et al.*, Physics of Plasmas **27**, 032703 (2020), https://doi.org/10.1063/1.5125599.

[181] D. S. Clark, C. R. Weber, J. L. Milovich,

et al., Physics of Plasmas **26**, 050601 (2019), https://doi.org/10.1063/1.5091449.

[182] M. Hohenberger, D. T. Casey, A. L. Kritcher, *et al.*, Phys. Plasmas **27**, 112704 (2020), https://doi.org/10.1063/5.0019083.

[183] J. E. Ralph, O. Landen, L. Divol, *et al.*, Phys. Plasmas **25**, 082701 (2018), https://doi.org/10.1063/1.5023008.

[184] N. Izumi, D. T. Woods, N. B. Meezan, *et al.*, PHYSICS OF PLASMAS **28**, 022706 (2021).

[185] H. Chen, D. T. Woods, O. S. Jones, *et al.*, Physics of Plasmas **27** (2020), 10.1063/1.5128501.

[186] H. F. Robey, L. Berzak Hopkins, J. L. Milovich, and N. B. Meezan, Phys. Plasmas **25**, 012711 (2018), https://doi.org/10.1063/1.5010922.

[187] J. S. Ross, J. E. Ralph, A. B. Zylstra, and Others, Nat. Commun. (2022), in preparation.

[188] J.-M. D. Nicola *et al.*, in *High Power Lasers for Fusion Research VI*, SPIE Proceedings, Vol. 11666, edited by A. S. Awwal, C. L. Haefner (2021).